Level Structures of ^{110,111,112,113}Rh from Gammasphere Measurements on ^{252}Cf

Y.X. Luo[1,2,3,4], S.C. Wu[4,5], J. Gilat[4], J.O. Rasmussen[4], J.H. Hamilton[1], A.V. Ramayya[1], J.K. Hwang[1], C.J. Beyer[1], S.J. Zhu[1,3,6], J. Kormicki[1], X.Q. Zhang[1], E.F. Jones[1], P.M. Gore[1], I-Yang Lee[4], P. Zielinski [4], C.M. Folden III[4], T.N. Ginter[4] P. Fallon[4], G.M. Ter-Akopian[7], A.V. Daniel[7] , M.A. Stoyer[8], J.D. Cole[9], R. Donangelo[10], S.J. Asztalos[11], and A. Gelberg[12]

[1] Physics Department,
Vanderbilt University,
Nashville, TN 37235,

[2] Institute of Modern Physics,
Chinese Academy of Science,
Lanzhou, China

[3] Joint Institute for Heavy Ion Research,
Oak Ridge, TN 37830,

[4] Lawrence Berkeley National Laboratory,
Berkeley, CA 94720,

[5] Department of Physics,
National Tsing Hua University, Hsinchu,
Taiwan

[6] Physics Department,
Tsinghua University,
Beijing 100084, People's
Republic of China

[7] Flerov Laboratory for Nuclear Reactions,
Joint Institute for Nuclear Research,
Dubna, Russia

[8] Lawrence Livermore National Laboratory,
Livermore , CA 94550,

[9] Idaho National Environmental and Engineering Laboratory, Idaho Falls, ID 83415,
[10] Instituto de Física da Universidade Federal do Rio de Janeiro, CP 68528, 21941-972 Rio de Janeiro, Brazil
[11] Massachusetts Inst. of Technology, Cambridge, MA 11830,
[12] Institut für Kernphysik, Universität zu Köln, 50937 Cologne, Germany

(Dated: August 24, 2003)

Abstract

Level schemes of ^{111}Rh and ^{113}Rh are proposed from the analysis of $\gamma - \gamma - \gamma$ coincidence data from a ^{252}Cf spontaneous fission source with Gammasphere. These schemes have the highest excitation energies and spins yet established in these nuclei, as well as weakly-populated bands not reported in earlier fission-gamma work. From these data, information on shapes are inferred. By analogy with lighter Z = 45 odd-even isotopes, tentative spins and parities are assigned to members of several rotational bands. In this region triaxial nuclear shapes are known to occur, and we carried out calculations for ^{111}Rh and ^{113}Rh with the triaxial-rotor-plus-particle model. The $7/2^+ \pi g_{9/2}$ bands of both nuclei, as well as lighter isotopes studied by others, show similar signature splitting. Our model calculations give a reasonable fit to the signature splitting, collective sidebands, and transition probabilities at near-maximum triaxiality with $\gamma \approx 28^\circ$. For the K=$1/2^+$ [431] band, experiment and model calculations do not fit well, which is accounted for by greater prolate deformation of the K=$1/2^+$ band, a case of shape coexistence. Our data on ^{110,112}Rh show no backbending and thus support the idea of the band crossing in the ground band of the odd-A neighbors being due to alignment of an $h_{11/2}$ neutron pair. In ^{111,113}Rh above the band crossing (spins $\approx$ 21/2~) the ground band appears to split, with two similar branches. We consider the possibility that chiral doubling may be involved, but there are not enough levels to determine that.

PACS number(s) : 21.10Re, 23.20.Lv, 25.85.Ca

I. INTRODUCTION

The fission-product Z=45 Rh isotopes are five protons below the 50-proton closed shell and mid-way in the 50-82 neutron shells. They are in a region where nuclei are characterized by shape co-existence, including triaxial shapes.[1] There has been considerable knowledge on the lower-spin level schemes from beta-decay studies of fission products, but we shall not try to review this except for relevant work more recent than the last Table of Isotopes [2], namely Lhersonneau et al.[3] on levels of ^{111}Rh and Kurpeta et al.[4] on levels of ^{113}Rh. Rather, we shall concentrate on the high-spin yrast or near-yrast levels directly populated by fission. In 1997 Gilat presented a paper [5] for our collaboration entitled "Prompt Gamma Emission by ^{136,137}I and ^{111,112,113}Rh Fission Fragments." The abstract of this paper notes transitions in ^{111}Rh (24 transitions, from 162 to 792 keV), in ^{112}Rh (8 transitions, from 61 to 621 keV) and in ^{113}Rh (11 transitions, from 212 to 718 keV). In 1999 Venkova et al.[6] published studies of ^{107,109}Rh isotopes from fission following fusion of ^{28}Si and ^{176}Yb. In 2002 Fotiades et al.[7] presented a paper with results of similar fusion-fission work with three different target-projectile combinations at Gammasphere. They showed in the conference abstract level schemes for ^{106,108,110,111,112}Rh and published in 2003. In 2002 Venkova et al.[8] published another paper on high-spin structure of ^{109,111,113}Rh isotopes. Our collaboration had shown preliminary level schemes for ^{111,112,113}Rh in a poster session at the INPC2001 conference [9], but these have not appeared in print. Thus, their fission-gamma level schemes and ours were developed independently of each other. They show good agreement on the main band, though our data reveal more bands and extra levels. We also have some disagreements, as will be discussed later. After seeing the ^{110}Rh level scheme of Fotiades et al.[7], we were able to extend it. We probably have better statistics than the others and are able to extend the bands higher in energy and spin.

In this paper, using our August and November 2000 multiple-coincidence ^{252}Cf spontaneous-fission Gammasphere data, we concentrate on the level structures of ^{111,113}Rh to extend the yrast/near-yrast level systematics for odd-even Rh isotopes from N = 62 through 68. Spin and parity assignments and configuration interpretations are proposed for the observed levels, and level schemes are presented. We also show data and present level schemes for the neighboring odd-odd isotopes ^{110,112}Rh. The level systematics and trends of level structure for Z=45 odd-even isotopes are discussed. Graphs of kinetic moments of in-

ertia vs. rotational frequency are shown to illustrate band-crossing features. Graphs of spin vs. rotational frequency are shown, and they facilitate the analysis of the particle alignment associated with the bands. The bands in odd-odd ^{110,112}Rh do not show any backbending (band crossing) up past the rotational frequency of backbending in the ground bands of the odd-even neighbors. Thus, we will argue that the backbending is likely the result of alignment of the $h_{11/2}$ neutrons.

For ground-band and collective side-band levels below the backbending we carried out model calculations with the quasi-particle+triaxial rotor model for a range of shape parameters, β and γ, thus deriving best-fit values for the shape parameters.

The odd-odd Rh isotopes are of great interest in that a similar high-spin band is seen across a large range of neutron numbers from ^{100}Rh with 55 neutrons, according to Duffait et al.[10] and Fotiades et al. [7], to ^{112}Rh with 67 neutrons. At the light end the bandhead is 8^- and likely attributable to the stretched-minus-one coupling of a half-filled $g_{9/2}$ proton subshell and an $h_{11/2}$ neutron. For 57 neutrons the bandhead becomes 6^-, slightly lower than the $8^-$and with a 7^- intermediate state. Fig. 10 of Duffait et al. [10] shows a similar behavior in the 47-proton Ag isotones. Above spin 10 the bands take on a more rotational character with generally increasing transition energies. The neutron-rich (N>56) nuclei of this region show bands indicative of deformed triaxial shapes or softness toward triaxiality. Indeed this high-spin isomeric band in the odd-odd nucleus ^{104}Rh appears [11] to show characteristics of chirality doubling proposed and developed theoretically by Frauendorf et al. [12]. Other examples put forth as chirality doubling are in the odd-odd N=75 isotones [13] and specifically for ^{135}Nd, an even-odd nucleus [14]. We will discuss these chiral bands further in the discussion section of this paper.

II. EXPERIMENT AND DATA ANALYSIS

It is clear that measurement with a fission source, spontaneous or induced, and with a multi-gamma detection array is a powerful method for studies of the high-spin structure of neutron-rich nuclei [15]. For two weeks each in August and November 2000 we made spontaneous-fission-gamma measurements in Gammasphere with 102 Compton-suppressed Ge detectors. A fission source of ^{252}Cf with a strength of 62 μCi, sandwiched between two Fe foils (10 mg/cm^2) was mounted in a 7.6 cm-diameter polyethylene ball centered in the

Gammasphere. More than 5.7×10^{11} triple and higher-fold events were accumulated. The Radware software uses all folds of three and higher to create a "Radware cube" of triple-coincidences [16].

We used typical (cf. Luo et al.[17]) methods of analysis of triple-gamma coincidence, double-gating first on known gamma transitions in the complementary fission fragments, in our case, Z=53 iodine, then cross-gating to include previously known transitions in the Rh nucleus. Finally, we did double-gating on transitions within the Rh nucleus of interest. An effort was made to determine transition energies and relative intensities as accurately as possible. The energy calibration was derived from known, well-determined (usually from beta decay studies of individual fission fragments as evaluated and cited in the 1996 Table of Isotopes[2]) energies of transitions in our own spontaneous-fission data set. These results are in good agreement with those determined from separate calibration measurements with familiar standards. Various double-gated spectra, generated using Radford's xmlev code [16] on the "cube" of triple-gamma coincidences from all folds of 3 or higher, were examined with the least-squares peak-fitting code "ft n" of Radford's gf3 program [16]. Transition energies and relative intensities were determined. For the different double gates showing a particular transition we made a weighted average of energy measurements to determine the final values of energy.

Tables I and II list the energies and relative intensities thus obtained for the assigned ^{111,113}Rh transitions, respectively. Tables III and IV are similar lists for ^{110,112}Rh transitions. From residuals of the energy calibration fit, a systematic error of ±0.1 keV is estimated. The statistical standard deviations except for the weakest peaks are probably less than this, but we are not able at present to obtain reliable values from the fitting programs, probably because of the data compression built into the standard Radware cube software that we used. (We hope eventually to be able to obtain and fit less compressed spectra and determine statistical standard deviations, resolve close-lying doublets, and examine line shapes for Doppler broadening.) We report two significant figures after the decimal point in the keV energy values because they may be useful in testing energy sums and differences in the proposed level schemes, even though the systematic standard deviation is probably around 0.1 keV. In our figures of level schemes, however, we round to the nearest 0.1 keV.

The tables also list transition energies reported in previous publications or conference contributions, one by our collaboration at the INPC 2001 conference in July 2001 [9], two

(2002 and 2003) by Fotiades et al.[7], and another by Venkova et al.[8]. Note that the first report of our collaboration (1997)[5] assigned 29 transitions to ^{111}Rh, whereas Table I lists 72, which are 43 and 35 more transitions assigned than in refs. [7],[8], respectively. Likewise, Gilat et al.[5] assigned 11 transitions to ^{113}Rh, whereas Table II lists 61 now. We find 48 more transitions in ^{113}Rh than reported in ref. [8]. In ^{112}Rh our 1997 report, Gilat et al.[5], assigned 8 transitions; Fotiades et al.[7]reported 10 transitions, whereas Table IV now lists 20. This illustrates the dramatic enhancement over six years in the spectroscopic knowledge on these isotopes. Our older work was based on a 1995 Gammasphere experiment, and the present paper makes use of a year 2000 Gammasphere experiment of more than three times the duration and with a complement of a third more Ge detectors.

Some transition energies from beta-decay work [3][4] are also listed in the tables, but only where they are also seen as prompt fission gammas in our fission work. In the above beta-decay work the energy uncertainties were listed as twice the standard deviation, which is about the 90% confidence level. We are generally in agreement with previously-reported energies within a standard deviation of energies from the beta-decay and fusion-fission work except for the strong transition from $9/2^+$to $7/2^+$ground state in ^{111}Rh. Lhersonneau et al. reported 211.4 keV, our earlier work posted at INPC2001 reported 211.7 keV, the fusion-fission work of Venkova et al.[8] gave 211.2 keV, and our Table 1 of this paper gives 211.70 keV. This discrepancy is not sufficiently large to upset any theoretical model comparisons, but it is instructive to examine the problem to try to understand it. Fortunately, there are a number of higher levels that decay to both the initial and final states of the $9/2^+$to $7/2^+$ground state transition, so we can compare differences and check. Table 5 lists such differences for all papers reporting energies to 0.1 keV. The 211.2(3) keV measurement of Venkova et al.[8] is within one standard deviation of the Lhersonneau et al.[3] direct value but lower than our measurement and differs from ours by nearly two standard deviations. It should be pointed out that our spontaneous fission work and the fusion-fission work suffers from possible interference with the nearly identical energy for the same transition in ^{113}Rh. Thus, it is necessary to take considerable care in setting the double gates. Although we probably have considerably better statistics than either of the fusion-fission studies, our direct value of 211.70 does seem a bit high. We then went back to redetermine a strong calibration point, the 2-0 transition in ^{100}Zr in the same fission-gamma data set. The Table of Isotopes reports an energy of 212.530(9) keV, and our redetermination gave

212.54 keV. It is worth noting that the energy values of ref.[8] for most transitions below 500 keV are systematically lower by around 0.5 keV compared to our values for the same transitions. Thus, we have not modified our own determinations in the data tables and for the level scheme. There are too many complexities of these rhodium spectra for the standard deviations on intensities to be meaningful, so they are not listed. Furthermore, there are several transitions so close in energy as to be unresolvable, and no intensity value is listed in a table. We estimate that the more intense transitions have intensity standard deviations of around 20% and the weaker transitions around 80%.

III. RESULTS AND DISCUSSION

A. Coincidence Spectra

Figs. 1, 2, 3, and 4 show a sample of the many double-gated coincidence spectra used to analyze these data. They are spectra from ^{111}Rh, ^{113}Rh, ^{110}Rh and ^{112}Rh, respectively. Transitions of these rhodium isotopes and their iodine fission partners are seen in the figures. When we began these rhodium studies several years ago, we had the advantage of prior knowledge of lower-spin states from beta-decay studies and close analogies with studies of lighter-mass rhodium isotopes. In the meantime there have appeared publications by other independent groups, as cited in the Introduction. We have been able to cross-check and build on their results or modify them.

B. Level schemes

By using the high statistics afforded by a month of Gammasphere running in year 2000 our collaboration has been able to enhance and extend our previous level schemes. With our transition-energy data of column 1 in Tables 1, 2, 3, and 4, we have used the least-squares program GTOL[18] to give a statistically optimum set of energy values for the levels of our proposed schemes, given in Figs. 5, 6, and 7 for ^{111}Rh, ^{113}Rh, and ^{110,112}Rh, respectively. The numbering of the bands follows that of Venkova et al.[6] for ^{107,109}Rh wherever possible.

1. ^{111}Rh

Band (1) of ^{111}Rh reaches 3933.4 keV, $(31/2^+)$ (α =-1/2) and 4249.3 keV, $(33/2^+)$ (α =+1/2). These are the highest spins and excitations so far observed in these neutron-rich Rh isotopes. Band crossings are thus clearly observed for the first time in both signature members of this $g_{9/2}$ band. Band (5) extends to 2905.1 keV $(23/2^+)$ level, and three levels of its α =+1/2 branch are newly observed for fission data. Band (6) reaching 2604.2 keV $(23/2^+)$ and band (7) reaching 3742.5 keV (29/2, 31/2) differ from those reported in [8]. Since the rotational sequence is built in band (6) up to the 2604.2 keV $(23/2^+)$ level, the 402.0 keV and 576.9 keV transitions definitely belong to band (6), which were reported to be decay-out transitions of band (7) in ref. [8]. Band (7) consists of two signature partners with four weak cross-over transitions identified. Thus, the bandhead of band (7) is 2112.7 keV (19/2, 21/2) level. The 1950.9 keV $(19/2^+)$ level shown in [8] as the bandhead of band (7) is found to be a level of band (6). Our fission data added two more levels, 1168.6 keV and 1758.2 keV, to band (3). Spin/parity asignments are based on the decay work [3, 4] for the low-lying levels and the assumptions of rotational sequences for those built on them. Spin 7/2 or 9/2 could be assigned to the new 1168.6 keV level of band (3). However, 9/2 is more likely, since a 7/2 level would be expected to decay also to the $3/2^-$ band member at 681.9 keV. Band (8), known from beta-decay work with two levels, is observed here for the first time using fission data.

Now look more closely at the differences between the level scheme of our Fig. 5 for ^{111}Rh and Fig. 3 of Venkova et al.[8], which is more extensive than that of Fotiades et al.[7]. They define a band (band 2) of two levels, decaying into the $25/2^+$ level of ground band (1), whereas we have those two levels, now with crossover transitions, as a continuation of band (1). The head of band (7) is now at 2112.7 keV. We have an additional weak transition from our designated bandhead of band (7), namely a 729.3-keV transition to the $17/2^+$ state of ground band (1). Our scheme requires there being two pairs of gamma rays that would be unresolvable in a singles spectrum, (576.4 and 576.9 keV) and (161.3 and 161.8 keV). We have, however, done careful background subtractions and used several combinations of double-gates to convince ourselves of the correctness of our level scheme. We also see four crossover transitions in band 7 not reported in ref. [8] but given in the 2002 abstract of ref. [7]. We assigned one more level, the spin $3/2^-$ of band (3) at 681.9 keV.There may be some

uncertainty in our relative intensities for those transitions in triple-cascades populated by beta decay, but we believe that the transitions in our level scheme of Fig. 5 all arise, for the most part, from prompt fission gamma transitions.

2. ^{113}Rh

The level scheme of ^{113}Rh is well developed in comparison with other reports and quite similar to that of ^{111}Rh. Venkova et al.[8] report (their Fig. 4) only band (1) to $(21/2^+)$ and band (6) to $(17/2^+)$ with only one depopulating transition, in contrast to our six-level band. All of their levels are confirmed except for their $(17/2^+)$ in band (6), where we do not observe their 476-keV transition. Band (1) of ^{113}Rh now reaches to $(31/2^+)$, almost the same excitation as does band (1) of ^{111}Rh. Band (6) now extends to 2398.5 keV $(21/2^+)$, with four weak crossover transitions identified. Bands (2), (5), (8), and possibly also band (3) are observed for the first time using fission data, previous reports having come from beta-decay work. Note that our spontaneous fission evidently populates this isotope more heavily than does the fusion-fission reaction from ^{18}O on ^{208}Pb.

Band (2) is remarkable in that its three upper levels are very close in energy to levels of the same spin in band (1). This behavior suggests it as a candidate for chiral doubling, but there is insufficient evidence. The only identified decay out of band (2) is to the $19/2^+$ level of band (1), and the multipolarity of the transition is undetermined. Thus, the parity could be negative if the transition were E1. The spins in band (2) could also be one unit higher if the transition were pure E2.

3. ^{110,112}Rh

Based on the work of Fotiades et al.[7], the level schemes of ^{110,112}Rh are extended to both higher- and lower-spin levels and cross-over transitions are identified in both nuclei. Three low energy transitions, 58.9 keV, 65.8 keV, and 60.6 keV, are observed. Total internal conversion coefficients (ICC) of these low-energy transitions were determined based on the intensity balance of two cascading transitions in spectra gated at the feeding transition above. From the ratio of photon intensities in the coincidence spectra we can determine total conversion coefficients if we know the multipolarity of one of the transitions. The only

consistent solution for ^{110}Rh is to assume the 58.9 keV transition at the bottom of the band to be E1, which has a theoretical total ICC of 0.665. From that we determine a total ICC of 1.49(5) for the 65.8-keV transition above it and 0.09(5) for the 159.3 keV transition above that. (The numbers in parentheses are rough statistical standard deviations.) From this we determine that the latter two transitions are mixed M1-E2 transitions. By gating on our Radware cubes with different time gates (TAC) we determine that the lowest transition, the 65.8 keV, has a half life of 16(4) ns, a retarded E1. By the same method in ^{112}Rh, assuming the 60.6-keV transition at the bottom of the band is E1 with theoretical total ICC of 0.614, we obtained a total ICC of 0.10(4) and 0.06(3) for the 159.2-keV and the 183.0-keV transition, respectively. The latter two transitions are thus also M1/E2 mixtures. Multipolarities of these low-energy transitions confirm the spin/parity assignments to the lowest-lying levels. The assignments for higher-spin levels are based on analogies to those of lighter isotopes.

C. Interpretations for the bands of ^{111}Rh and ^{113}Rh

The most prominent feature in both nuclei is the ground band (1), where we show the two signature partners horizontally displaced for clarity. This band is quite similar in both nuclei. The lowest transition is nearly identical in energy for the two nuclei, and higher-level spacings are also similar. The sign of the signature splitting is that expected for a band based on an odd $g_{9/2}$ proton. As we shall discuss in a later section, the signature splitting of bands (1) and (6) is indicative of a shape slightly on the prolate side of maximal triaxiality. The cascade transitions are of comparable intensity to the competing cross-over transitions. We cannot use the simple Clebsch-Gordan branching ratios for E2 transitions where the angular momentum projection K is a good quantum number, since the nuclear shape for band (1) is so triaxial as to cause considerable K-mixing. For ^{111}Rh and ^{113}Rh we have neither internal conversion nor angular correlation data to determine the M1/E2 ratios in the cascade transitions. However, for the low-energy transitions at the bottom of the main bands in ^{110}Rh and ^{112}Rh we have been able to measure total ICC and determine multipolarities and a lifetime, as we discussed above. For the odd-A isotopes the raw cascade-to-crossover intensity ratios make it likely that the cascades are predominantly M1. The strong M1s are to be expected given the fact that the odd $g_{9/2}$ proton will have a much larger magnetic

g-factor than the collective rotation g-factors. In both nuclei there is a backbending that sets in above the 21/2 level (^{111}Rh) or the 19/2 level (^{113}Rh). Fig. 8 is a backbending plot (kinetic moment-of-inertia vs. rotational frequency) for the Rh nuclei studied here, where we have included ^{109}Rh from Venkova et al.[6], augmented by one additional higher transition we measured, establishing the backbending point for ^{109}Rh. The backbending frequency moves monotonically lower with increasing neutron number. The lack of backbending in our ^{112}Rh main band, where there would be blocking by an odd neutron, suggests that the backbending signifies a neutron pair breaking in the odd-A isotopes of Rh. Comparison with nearby even-even and even-odd nuclei suggests that the pair breaking is in the $h_{11/2}$ orbital, since the backbending frequency and aligned angular momentum is comparable to that in the odd-even rhodiums. This suggestion is also supported by the aligned angular momentum, which is deduced from Fig. 9.

Next we call attention to bands (6) and (8) . In both odd-A nuclei that we studied bands (6) have $11/2^+$ bandheads close in energy to the $11/2^+$ excited level in the ground bands (1). The $3/2^+$ bandheads of bands (8) lie even lower. At first we thought of bands (6) and (8) as gamma-vibrational bands. However, one notes a strange behavior in that the band (6) bandheads have a very weak E2 transition to the ground state. Band (8) decays by enhanced E2 to the ground state. We claim that bands (1), (6), and (8) are a collective family with triaxial deformation. The triaxiality produces much K-mixing and different transition branching ratios from those in purely spheroidal nuclei. In the analysis of Gelberg et al.[19] on ^{125}Xe the signature pattern of the yrast band could be matched by two triaxial shapes, one on the prolate side and another on the oblate side. The yrare band was used to decide between triaxial solutions on prolate and oblate sides of maximum triaxiality. In the xenon case the side band analogous to our $11/2^+$ had a very weak signature splitting, and of an opposite sign to that of the main band. They simply called it the yrare band. In the odd-A rhodiums the $11/2^+$ yrare bands both have weak signature splitting of opposite sign to the main band. In our model calculations in a later section we show the signature splitting, band head energies, and branching ratios for the odd-A rhodium isotopes are natural consequences of the triaxial shape, slightly on the prolate side.

Bands (6) and (8) we would suggest are collective bands associated with the ground band and the strongly triaxial shape; they would correlate to gamma vibrational bands in the axially symmetric limit. Lhersonneau et al.[3] in their Table 4 show E2 transitions from

band (8) to the ground band enhanced by factors of six or more over the single-particle lifetimes. This strongly suggests that bands (8) and (1) are in a collective family. Before presenting our computer modeling results for a single quasiproton in a triaxial well, it may be useful to look at rotational moments-of-inertia within the old model of an odd-proton hole coupled to a prolate spheroidal core, ignoring the K-mixing induced by the triaxiality. The rotational energy may be written as

$$E(I, K_{tot}, K_{gam}) = A_{perp} \left[I(I+1) - K_{tot}^2 \right] + A_{par} K_{gam}^2, \quad (1)$$

where I is the total angular momentum, K_{tot} is the total projection on the long (cylindrical) axis, K_{gam} is the collective (rotational) angular momentum along the long axis, and A_{perp} and A_{par} the rotational constants perpendicular and parallel to the long axis, respectively. We omit a rotational energy term that is the same in all members of the bands in a collective family $A_{perp}\,[j(j+1) - \Omega^2]$, where j is the particle (hole) angular momentum, in this case 9/2, and Ω is its projection on the long axis, here 7/2. Therefore, our first-order calculation using Eq.(1) estimates the rotational constants A_{perp} from the spacing between ground and the average of the two lowest 11/2 states, assumed degenerate before mixing. We get A_{perp} of 27.5 keV for ^{111}Rh and 25.4 keV for ^{113}Rh. It is easy to show from Eq. (1) that degeneracy dictates a ratio of $A_{par}/A_{perp}$of 4.5, independent of particle j. For comparison the even-even triaxial nucleus ^{106}Mo, based on the energies of the first two 2^+states and Eq.(1), has A_{perp} of 28.6 keV and a ratio A_{par}/A_{perp} of 5.7. If we apply Eq.(1) and these rotational constants to calculate the energy of the first $3/2^+$ state, the energies come out too high ($>$ 400 keV.) However, the triaxial rotor model calculations we present later show the $3/2^+$ band (5) at about the energy observed experimentally.

Band (5) is well populated in ^{111}Rh up to spin $23/2^+$, but only levels up to $9/2^+$ are seen in ^{113}Rh. This irregularly-spaced K=1/2 band in ^{107}Rh has been nicely fitted by Venkova et al.[6] and shown in their Fig. 10. Kurpeta et al.[4] in their Table 3 give a fit for this band in both ^{111}Rh and ^{113}Rh. Their best fit parameters are rotational constants of 19.6 keV and 20.0 keV, respectively, and staggering (decoupling) parameters of -33.65 keV and -26.83 keV, respectively. Lhersonneau et al.[3] measured lifetimes of the analogous bandhead in the ^{109,111}Rh isotopes to show E2 transitions to ground $7/2^+$ as retarded. This information makes clear that band (5) is the intruder state 1/2[431] from the major shell above. The decoupling parameter indicates $g_{7/2}$ predominating over $d_{5/2}$ in the composition of this odd-

proton state. This intruder orbital is strongly prolate-driving, and thus we would expect the total deformation of this band to be greater than that of the other bands, another case of shape coexistence.

In ^{111}Rh our data reveal five levels of a K=$1/2^-$ band, designated band (3). The beta-decay work of Lhersonneau et al.[3] shows the lowest three levels of this band, and they measured the half life of the $1/2^-$ bandhead at 492.9 keV as 6.8(4) ns. They calculate that this half-life corresponds to 6.5 x 10^{-6} single-particle units for E1 decay to the $3/2^+$ bandhead of the K=3/2 band at 303.7 keV. The K=$1/2^-$ band is probably the prolate 1/2[301] band. The spacing is irregular, as usual, for K=1/2 bands with close-lying 3/2 and 5/2 members. If the band were pure $p_{1/2}$, the 3/2 and 5/2 would be degenerate. As discussed in Sec. 4.2.2 of Lhersonneau et al.[3], the 3/2 and 5/2 were also measured in earlier studies. Some admixture of $p_{3/2}$ and $f_{5/2}$ into band (3) is to be expected and would account for breaking the doublet degeneracy of the 3/2 and 5/2 members. There are too few known levels in this band to determine possible triaxiality. In ^{113}Rh we tentatively assign one level at 785.1 keV to band (3), the 1/2[301] band, but the spin and band assignment is uncertain. Extrapolation from the level systematics Fig. 4 of Lhersonneau et al.[3] supports this idea. Earlier authors sometimes discuss band (3) as a spherical coupling of $p_{1/2}$ proton with core vibrational states. Our identification of the 1168.6- and 1758.2-keV states in ^{111}Rh as members of the band would argue more for a spheroidal shape, since the band spacings are not constant but increasing with spin.

Band (7) in ^{111}Rh and band (2) in ^{113}Rh we originally assigned in analogy to bands of those numbers in the lighter rhodiums identified in the work of Venkova et al.[6] It seems likely that these are three-quasiparticle bands closely related to the ground band (1) and yrare band (6), into which they feed. The close proximity of levels of the same spin and parity raise the intriguing question whether the bands could partly be chiral doublets of the part of bands (1) above the backbend.

D. Level systematics of the Z = 45 odd-even isotopes

Fig. 10 shows the systematics of rotational spacings in band (1) in odd-A rhodiums from mass 107 through 113. This is an extension of the ground-band part of Fig. 4 of Lhersonneau et al[3]. There seems to be a great similarity, with gradually decreasing spacing

as the mass number increases. The smooth evolution of the levels with changing neutron numbers supports the spin/parity assignments. In ^{107}Rh the measurements do not go high enough to observe the backbending, but the systematics of the other three nuclei show a monotonic lowering of the backbending frequency as the mass increases.

IV. TRIAXIAL-ROTOR-PLUS-QUASIPARTICLE MODEL CALCULATIONS

A. The model

Although a superficial look at the yrast cascades of $^{111-113}$Rh seems to indicate strong coupling, the large signature splitting and a few unusual gamma branching ratios point to the presence of triaxial deformation. To see whether at least the properties of the yrast states of band (1) below the backbend, a few yrare states in band (6), and the collective sideband (8) can be described by the rigid triaxial-rotor-plus-particle model [20–22] we tried calculations based on this model. Triaxial-rotor-plus-particle calculations for ^{107}Rh have also been carried out in [6]. The details of the model we used can be found in [21]. We will only sketch the main features of the model. The nuclear shape is described by the conventional deformation parameters β and γ [23]; we did not assume a hexadecapole deformation. The rotor plus particle Hamiltonian is

$$H = H_{sp} + H_{pair} + \sum_{k=1,2,3} \frac{\tilde{}^2}{2\Theta_k}(I_k - j_k)^2, \tag{2}$$

where H_{sp} is the single-particle Hamiltonian in a triaxially deformed mean field and H_{pair} is the pairing Hamiltonian. **I** and **j** are the total and particle angular momenta, respectively. The hydrodynamical moments of inertia

$$\Theta_k = \Theta_0 \frac{4}{3} sin^2(\gamma + \frac{2\pi}{3}k) \tag{3}$$

have been used. The so called Lund convention for (β, γ) is used [21]. In order not to confuse the reader, the parameters given in the results of the fit respect the more widely used "Copenhagen" convention, according to which $\beta \geq 0$ and $0 \leq \gamma \leq 60°$ define the shape of a triaxial rotor with collective rotation. The triaxial rotor is called "rigid" because β and γ are constant throughout the calculation (c-numbers) or, in other words, there is no vibrational motion. As a consequence, the core has no excited 0^+ state. Although the codes

employed in this work [24, 25] allow the use of variable moments of inertia [20], in order to reduce the number of free parameters, we used only a constant moment of inertia. The basis states of the Hamiltonian (1) are [23]

$$|IMK\nu\rangle = \sqrt{\frac{2I+1}{16\pi^2}}(D^I_{MK}\phi_\nu + (-1)^{I+K}D^I_{M-K}\tilde{\phi}_\nu) \tag{4}$$

where ϕ_ν is the single-particle wave function. It contains Nilsson orbitals with different values of the particle projection quantum number Ω. Due to the triaxial deformation, Ω and the projection K of the total angular momentum I are not good quantum numbers and $K \neq \Omega$; $\tilde{\phi}$ is the time reversal conjugate of ϕ. The single-particle states are the eigenfunctions of a deformed harmonic oscillator potential. We used the so called stretched intrinsic coordinates [26]. The standard Nilsson parameters μ and κ [24] have been used. The single-particle basis contains 15 deformed basis states (Nilsson orbitals). They include all the Nilsson orbitals originating from $1g_{9/2}, 1g_{7/2}, 2d_{5/2}$ and $2d_{3/2}$. Pairing is introduced via standard BCS. The Fermi energy and the pairing gap are determined as functions of the isoscalar and isovector pairing strengths [23], i.e. they are not free parameters. The model contains also a Coriolis attenuation factor. The model is able to calculate E2 and M1 transition matrix elements. Only the core contribution to B(E2) is considered. In the M1 calculation the spin g-factor is quenched by a factor of 0.75.

B. Results

The main fit parameters are the deformation parameters β and γ and the energy of the first excited core state $E(2^+)$. The latter is equivalent to the moment of inertia parameter Θ_0. It would of course be naive to take $E(2^+)$ just equal to the excitation energy of the closest Ru or Pd core, since a quasiparticle is a mixture of a particle and a hole state. Besides, we may expect that the core is polarized by the last valence particle. The parameters β, γ and $E(2^+)$ have been fitted to the excitation energies and to several important branching ratios. The Coriolis attenuation has been fixed at $\xi = 0.8$. The usual values of the pairing parameters $GN_0 = 19.2$ and $GN_1 = 7.4$ have been taken. No effective charge for E2 transitions has been considered. During the fit particular attention has been paid to the signature splitting function S(I), which is extremely sensitive to γ. This function is defined as

$$S(I) = \frac{E(I) - E(I-1)}{E(I) - E(I-2)} \cdot \frac{I(I+1) - (I-2)(I-1)}{I(I+1) - (I-1)I} - 1 \tag{5}$$

We explored the $\beta - \gamma$ plane for several plausible values of $E(2^+)$. We tried to achieve an acceptable compromise in reproducing the absolute values of the excitation energies, the signature splitting and several branching ratios. As mentioned in section III.C, the small value of $B(E2; 11/2_2 \rightarrow 7/2_1)$, the transition from the bandhead of yrare band (6), is a peculiar feature of both investigated nuclei, as well as lighter mass odd-A nuclei. Therefore, we tried to obtain a good fit of the branching ratios of the yrare $11/2_2^+$ states. The fitted parameters are $E(2^+) = 0.31MeV, \beta = 0.28$ and $\gamma = 28^\circ$ for ^{111}Rh and $E(2^+) = 0.3MeV, \beta = 0.27$ and $\gamma = 28^\circ$ for ^{113}Rh. The half-life of the 9/2 state at 212 keV in ^{113}Rh, namely $T_{1/2} = 0.21(13)ns$ is given in [4], with a conversion coefficient $\alpha_K = 0.06$. A $B(E2; 9/2_1 \rightarrow 7/2_1) = 100$ WU was extracted. Our calculation predicts B(E2)=86 WU. This shows that our choice of β was realistic. As expected, the parameters for the two Rh isotopes are nearly the same. A comparison of theoretical and experimental excitation energies of ^{111}Rh and ^{113}Rh can be seen in figs. 11 and 12, respectively. The fit of yrast states in both nuclei is rather good, although there are a few discrepancies. In ^{113}Rh, in which several yrare states are known, the fit is satisfactory up to $15/2_2$, but the theoretical energies of higher-lying states are too large. Anyway, we should keep in mind that we deal with a one quasiparticle model, so that the calculation is valid only below the backbending region. The signature splitting function for the two nuclei can be seen in figs. 13 and 14. A better fit of S(I) would have been obtained for slightly smaller values of γ, but the agreement of the other observables would have deteriorated. One can notice an anomaly at the beginning of the experimental signature splitting plot of ^{113}Rh (fig. 14). The value of S(I) for $I = 13/2$ is very small, in contrast to ^{111}Rh. The branching ratios are shown in Table VI. The model reproduces only roughly the branchings in ^{111}Rh, while the agreement is better in the case of ^{113}Rh. The weakness of the $11/2_2 \rightarrow 7/2_1$ transition is satisfactorily reproduced in both nuclei. We can understand the reason for this quenching by examining the wave functions. It happens that the main core component in the wave functions of both the initial and final states is the 2_1^+ core state. Therefore, the E2 transition strength is mainly dictated by the diagonal E2 reduced matrix element, which vanishes for $\gamma = 30^\circ$. On the contrary, the main core component of the $9/2_1$ state is the 0^+ state of the core, therefore $B(E2; 11/2_2 \rightarrow 9/2_1)$ is large. As a rule, transitions between the unfavored yrare and unfavored yrast levels are hindered . For instance, in ^{111}Rh, the model calculation gives $B(E2; 15/2_2 \rightarrow 11/2_1) = 8e^2fm^4$. For the sake of compari-

son, $B(E2; 15/2_2 \rightarrow 13/2_1) = 44e^2fm^4$ and $B(E2; 15/2_2 \rightarrow 13/2_2) = 2048e^2fm^4$. This effect is also a signature of the triaxial deformation [22]. A general feature of the $\Delta I = 1$ transitions between yrast states with opposite signatures is the clear M1 dominance. If we examine the single-particle structure of the wave functions, we notice that most yrast states are dominated by components with K=7/2. The strongest component of the intrinsic wave function of the band-head is the $|nlj\Omega\rangle = |44\frac{9}{2}\frac{7}{2}\rangle$ Nilsson orbital (asymptotic quantum numbers $[413]\,\frac{7}{2}$). This explains why the level scheme looks so much like strong-coupling to a spheroidal shape. As far as the yrare states, band (6), are concerned, the lower ones are dominated by K=11/2, but the structure changes gradually when we go higher in spin. In both nuclei we notice the presence of low lying $3/2^+$ states (band-heads). In ^{111}Rh, as mentioned above, the $3/2^+$ state at 395 keV belongs to a K=1/2 band. Our calculation shows such a K=1/2 band based on the $[431]\,1/2^+$ orbital. The $3/2^+ \rightarrow 7/2^+$ transition to the ground band is strongly hindered [3]. The calculation gives $B(E2; 3/2 \rightarrow 7/2) = 6e^2fm^4$, which is at least two orders of magnitude smaller than for the strong E2's. However, the experimental value is $B(E2) = 0.40(6)e^2fm^4$, i.e. the transition is further hindered by one order of magnitude. Moreover, the fit of the excitation energies of this band is not good. These features are in agreement with the hypothesis that this band has a different deformation (see section III.C). A band with the $3/2^+$ band-head at 263.2 keV is present in ^{113}Rh. According to the calculation, the $5/2^+$ state of the band could not be populated if it were dominated by $K = 1/2$. The calculation shows a $3/2^+$ band-head with $K_{dom} = 3/2$, which has the same main intrinsic component as the ground state with $K_{dom} = 7/2$. This intrinsic configuration is $[413]\,\frac{7}{2}$. This unexpected feature is due to the different alignments of the core rotational angular momentum. (In a quantum-mechanical triaxial rotor, the angular momentum must not be oriented along an intrinsic axis). If we look at the projection R_3 of the core angular momentum on the quantization axis, we find that $\sqrt{\langle R_3^2\rangle}$ has the values 1.87 for the $3/2^+$ state and only 0.59 for the ground state. This is consistent with the above interpretation. As a matter of fact, the states of the yrare band with $K_{dom} = 11/2$ also have an intrinsic particle configuration with $[413]\,7/2$ as the main component. The question may be asked whether the fitted values of the deformation parameter γ are unique. In the case of odd-A Xe and Ba isotopes [19] the yrast signature splitting was correctly described not only for $\gamma \approx 24°$, but also for a value situated in the $30° \leq \gamma \leq 60°$ interval. However, the yrare signature splitting was correctly described only by the lower value of γ, and thus the

ambiguity was removed. In order to answer this question, we started increasing γ in the calculation of ^{111}Rh. At the beginning, this led to a deterioration of the signature splitting. At $\gamma = 36^\circ$ the $9/2^+$ state became ground state. We managed to bring back the ground state at $7/2^+$ by increasing the β deformation, but the signature splitting got even worse. Increasing β to 0.4 did not help. We did not try to further increase β to physically unrealistic values. This procedure was repeated for $\gamma = 40^\circ, 50^\circ$ and 60°, respectively, and the result was always the same. Apparently, the data cannot be fitted with $30^\circ \leq \gamma \leq 60^\circ$. A final remark concerning the deformation parameter γ: the idea of rigid deformation is a bit too simple. The properties of non-axially- symmetric nuclei are better described by gamma-soft models. It has been proposed to consider the fitted value of γ as an effective parameter [27].

C. Possible Chiral Doubling Effects in ^{111}Rh and ^{113}Rh

Above spin 21/2 in the ground bands of ^{111}Rh and ^{113}Rh there is a backbending (band-crossing) continuing at higher spins as two bands. One branch we have somewhat arbitrarily labeled as band (1). The other in ^{111}Rh is labeled band (7). There are similarities in ^{113}Rh, but there are fewer levels above the backbend. If these higher bands showed a spacing pattern in which the members of the same spin systematically approached degeneracy with increasing spin, we might think that they constituted a chiral doubling, as defined by Frauendorf[12]. While the best candidates for chiral doubling are odd-odd nuclei, we have the theoretical conditions for chirality in the 3-quasiparticle bands with a $g_{9/2}$ proton (hole) and aligned $h_{11/2}$ neutron (particle) pair within a triaxial well. That is, the proton hole angular momentum should align along the longest axis, the neutron pair along the shortest axis, and the rotational angular momentum along the axis of intermediate length, along which the moment-of-inertia is greatest. The chiral doubling is by no means the only way to generate such similar high-spin bands. With three large particle-angular-momentum vectors and a rotational-angular-momentum vector there are many slight changes in coupling that can generate close-lying levels with the same spin and parity. The chiral doubling may thus be obscured by configuration mixing of many couplings.

V. INTERPRETATIONS OF ODD-ODD RHODIUM ISOTOPES 110 AND 112.

We have been able to identify only one band in ^{110}Rh and a very similar band in ^{112}Rh, plus a sideband of two members. Above the 8^- level there is a remarkable series of similar bands in odd-odd rhodium and in silver isotopes all the way down to 55 neutrons, close to the 50-neutron closed shell. See Fig. 10 of Duffait et al.[10]. Fotiades et al.[7] measured heavier odd-odd rhodiums up through ^{112}Rh, showing the similarities of this band with spacings gradually decreasing with mass number. Duffait et al.[10] show a continuation of the band for two transitions below spin 8. Fotiades et al.[7] showed only the transitions above spin 8. We show in our level scheme three lower-energy transitions below spin 8 for ^{110}Rh and two for ^{112}Rh. With the new crossover transitions the bands in ^{110,112}Rh have a different appearance.

The band at higher spins is thought to be a case where an odd $g_{9/2}$ proton and odd $h_{11/2}$ neutron and the core collective angular momentum are all aligned. The structure problem is complicated by the fact that the $g_{9/2}$ proton orbital is about half-filled at Rh (Z=45.) The $h_{11/2}$ neutron orbital is unfilled up to N=70 for spherical shape and somewhat filled for spheroidal shapes. Explaining the persistence of a baseline spin 8 in a spherical basis might need a spin 7/2 configuration of three proton holes in the $g_{9/2}$, with the particle-hole coupling giving one less than the maximum spin lowest in the multiplet of coupling a 7/2 vector with an 11/2 vector. We shall not here further speculate on spherical-basis coupling schemes. The heaviest nuclei of the series surely are deformed, probably prolate spheroidal with uncertain triaxiality. The Table of Isotopes [2] shows for ^{110}Rh that there is beta decay from two isomeric states, with ground state undetermined. The higher-spin state is denoted as spin (≥ 4). The best constraint on the spin is a beta decay branch with log ft of 5.8 to a 3^- state, and this would not seem to permit a spin higher than 4. Thus, it is possible that the lowest level in our level scheme for ^{110}Rh can be this state. The same considerations apply to ^{112}Rh, except that no beta decay branch goes to a daughter state with definitely claimed spin, and we are left with the Table of Isotopes [2] tentative assignment of (≥ 4). Let us look at the level diagram of Skalski et al.[1] in the prolate region for high-j orbitals that might make up the band we observe in the odd-odd nuclei. The proton candidate is the $7/2^+[413]$. The neutron orbital would be $5/2^-[532]$. Those orbitals would make a $K=6^-$ bandhead. One would expect that such a band might barely start with regular I(I+1) level

spacing above which the j vectors would align. That could produce a band with very close spacing at the bandhead. There is, however, no clear interpretation of the level scheme, as it stands. Fig. 15 shows the signature splitting of the odd-odd rhodium isotopes here studied. As is often observed in similar cases, there is a reversal of sign in the signature splitting going up the band in ^{112}Rh. The ^{110}Rh is similar, but its band is not observed high enough to see the reversal. That would suggest to us at the upper end of the band that Coriolis coupling (highly spin-dependent) into an irregularly spaced K=0^- band dominates and at the lower end a spin-independent Y_{22} coupling term from triaxial deformation or soft vibration dominates to couple into a K=0^- with opposite signature splitting to the one reached by Coriolis coupling. The np force between the odd nucleons should not couple states of different K, but they can couple states in which the projection quantum numbers Ω and parities of the odd-nucleon orbitals simultaneously change, keeping an overall K and parity the same. So far as we know there have been no theoretical studies with a two-quasiparticles+triaxial core model, but there is such work with an axially symmetric core, R. Zheng et al.[28] and references therein.

VI. SUMMARY

We have proposed near-yrast level schemes for ^{111}Rh and ^{113}Rh, finding many similarities and some differences from earlier literature on ^{107}Rh and ^{109}Rh. Further evidence of shape coexistence in Rh isotopes is provided from the high-statistics fission-gamma data of the present work. From comparing energies and relative intensities with model calculations we determined that the lowest bands of these odd-even rhodium nuclei are triaxial, namely, $\gamma \approx 28$ degrees, but slightly on the prolate side. The very small values of $B(E2; 11/2_2 \rightarrow 7/2_1)$ also indicate triaxiality. The signature splitting in the Rh ground (yrast) and yrare bands are similar to the case of ^{135}Xe analyzed earlier[19]. We have observed band-crossing (backbending) with both branches above the crossing observed in ^{111}Rh and ^{113}Rh, and we have added one higher transition to ^{109}Rh, showing the beginning of a band-crossing there also. We propose that backbending results from alignment of a neutron pair from the $h_{11/2}$ orbital. Above the backbend the two branches show a closeness of levels of the same spin and parity. This is a hint of possible chirality effects, though configuration mixing may make a firm determination unlikely.

For the odd-odd rhodium nuclei the work of Fotiades et al.[7] and the work here reported, only one band is observed, analogous to a high-spin isomeric (8^-) band observed to as low mass number as 102. We report some lower-energy transitions below the 8^- level and determine their multipolarities from total conversion coefficients. We also measure a half life for an E1 transition. The dynamic moment-of-inertia above this alignment is nearly the same in ^{110}Rh and ^{112}Rh as in the odd-even neighbors ^{111}Rh and ^{113}Rh. However, the odd-odd bands do not exhibit any higher band crossing up to frequencies above where the odd-even neighbors backbend. This behavior supports the idea that the band crossing in the odd-even nuclei is due to alignment of a neutron pair from the $h_{11/2}$ orbital.

VII. ACKNOWLEDGMENTS

The work at Vanderbilt University, Lawrence Berkeley National Laboratory, Lawrence Livermore National Laboratory, and Idaho National Engineering and Environmental Laboratory are supported by U.S. Department of Energy under Grant No. DE-FG05-88ER40407 and Contract Nos. W-7405-ENG48, DE-AC03-76SF00098, and DE-AC07-99ID13727. The Joint Institute for Heavy Ion Research is supported by its members, U. of Tennessee, Vanderbilt, and the U.S. DOE through contract No. DE-FG05-87ER40311 with U. of Tennessee.The work at the Joint Institute for Nuclear Research in Dubna, Russia, is supported in part by the U.S. Department of Energy contract DE-AC011-00NN4125, BBW1 Agreement No. 3498 (CRDF grant RPO-10301-INEEL) and by the joint RFBR-DFG grant (RFBR No. p2-02-04004, DFG No. 436RUS 113/673/0-1(R)). The work at Tsinghua University in Beijing is supported by the Major State Basic Research Development Program under Contract No. G2000077400 and the Chinese National Natural Science Foundation under Grant No. 19775028.

The authors here are indebted for the production of ^{252}Cf to the Office of Basic Energy Sciences, U.S. Department of Energy, through the transplutonium element production facilities at the Oak Ridge National Laboratory. The authors would also like to acknowledge the essential help of I. Ahmad, J. Greene and R.V.F. Janssens in preparing and lending the ^{252}Cf source used in the year 2000 runs. Dr. K. Gregorich was instrumental in design of the source holder and surrounding plastic absorber ball and in mounting the source. Dr. A. Macchiavelli provided valuable help in setting up the Gammasphere electronics for data

taking. The authors would like to thank Prof. I. Ragnarsson and Prof. P. Semmes for kindly providing the computer codes for triaxial nuclei and for stimulating discussions. Ms. I. Stefanescu's valuable help on the theoretical model calculations is acknowledged with thanks.

---

[1] J. Skalski et al., Nucl.Phys. **A 617**, 282 (1997).

[2] R.B. Firestone and V.S. Shirley, Table of Isotopes, 8th ed. (John Wiley and Sons, Inc., New York, 1996) and CD-ROM 1998 Update.

[3] G. Lhersonneau et al., Eur. Phys. J. **A 1**, 285 (1998).

[4] J. Kurpeta et al., Eur. Phys. J. **A 13**, 449 (2002).

[5] J. Gilat et al., Bull. Am. Phys. Soc. **42**, 1658 (1997).

[6] Ts. Venkova et al., Eur. Phys. J. **A 6**, 405 (1999).

[7] N. Fotiades et al., Abstract for "Triangle Conference", Grand Tetons, Wyoming, May 2002, also Phys. Rev. **C 67**, 064304 (2003).

[8] Ts. Venkova et al., Eur. Phys. J. **A 15**, 429 (2002).

[9] J. Gilat et al., poster presentation at the Int. Nucl. Physics Conf. 2001, Berkeley, CA, July 2001.

[10] R. Duffait et al., Nucl. Phys. **A 454**, 143 (1986).

[11] T. Koike et al., "Conference on Frontiers of Nuclear Structure" July 29-August 2, 2002, abstract book, LBNL Report-50598 Abs., p. 30.

[12] S. Frauendorf and J. Meng, Nucl. Phys. **A 617**, 131 (1997); V.I. Dimitrov, S. Frauendorf, and F. Dönau, Phys. Rev. Lett. **84**, 5732 (2000), S. Frauendorf, "Conference on Frontiers of Nuclear Structure" July 29-August 2, 2002, abstract book, LBNL Report-50598 Abs., p. 15. cf. also S. Frauendorf, Rev. Mod. Phys. **73**, 463 (2001).

[13] K. Starosta et al., Phys. Rev. Lett. **86**, 971 (2001); "Conference on Frontiers of Nuclear Structure" July 29-August 2, 2002, abstract book, LBNL Report-50598 Abs., p. 148.

[14] S. Zhu et al.,"Conference on Frontiers of Nuclear Structure" July 29-August 2, 2002, abstracts, LBNL Report-50598 Abs., p. 148.

[15] J.H. Hamilton et al., Prog. Particle and Nucl. Phys. **35**, 635 (1995).

[16] D.C. Radford, Nucl. Instrum. Methods Phys. Res. **A 361**, 297 (1995), also cf. his website

http://radware.phy.ornl.gov/.

[17] Y.X. Luo et al., Phys. Rev. **C 66**, 014305 (2002).

[18] Program GTOL Version 6.4a T.W. Burrows, Brookhaven National Lab, Upton, NY (July 11, 2001, unpublished) (Original authors: W.B. Ewbank, B.J. Barton, L.P. Ekstrom, and P. Andersson.)

[19] A. Gelberg et al., Nucl. Phys. **A557**, 439c (1993).

[20] H. Toki and A. Faessler, Nucl. Phys. **A253**, 231 (1975).

[21] S. E. Larsson, G. Leander and I. Ragnarsson, Nucl. Phys. **A307**, 189 (1978).

[22] I. Hamamoto, Nucl. Phys. **A520**, 297c (1990).

[23] A. Bohr and B. R. Mottelson, Nuclear Structure, vol II, W. A. Benjamin, Reading, Mass., 1975

[24] I. Ragnarsson and P. Semmes, code GAMPN1 (1999, unpublished).

[25] I. Ragnarsson and P. Semmes, codes ASYRMO and PROBAMO (1991, unpublished).

[26] S. E. Larsson, Phys. Scripta **8**, 17 (1973).

[27] T. Yamazaki et al., Journ. Phys. Soc. Jap. **44**, 1421 (1978).

[28] R. Zheng et al., Int. Jour. Mod. Phys. **E 12**, 59 (2003), Phys. Rev. C 56, 175 (1997).

Figure captions

Fig. 1. A double-gated, triple-coincidence gamma spectrum for ^{111}Rh analysis.

Fig. 2. A double-gated, triple-coincidence gamma spectrum for ^{113}Rh analysis.

Fig. 3. A double-gated, triple-coincidence gamma spectrum for ^{110}Rh analysis.

Fig. 4. A double-gated, triple-coincidence gamma spectrum for ^{112}Rh analysis.

Fig. 5. Proposed level scheme for ^{111}Rh. We include only levels populated by prompt gamma rays following spontaneous fission of ^{252}Cf. That is, we do not show levels and transitions assigned from beta-decay studies alone. The prompt gamma spectra generally populate yrast and near-yrast levels, in contrast to beta decay.

Fig. 6. Proposed level scheme for ^{113}Rh. See Fig. 5 legend for further remarks.

Fig. 7. Proposed level scheme for ^{110,112}Rh. See Fig. 5 legend for further remarks.

Fig. 8. Band-crossing (backbending) plot for ^{109,111,113}Rh, that is, kinetic moment-of-inertia vs. frequency. The plot is for the +1/2 signature partners in all cases. Data for ^{109}Rh are from induced-fission-gamma work in Eurogam, except for our one additional transition at the top of the band. Note that the band crossing tends toward lower frequencies as the mass number increases.

Fig. 9. Plot of spin vs. frequency for ^{111,113}Rh ground band +1/2 signature partner. This type of plot shows about 8 units of aligned angular momentum from the spin displacement at the middle of the backbend. We believe the data confirm the idea that it is alignment of a neutron pair in the $h_{11/2}$ orbital that is responsible for the band-crossing.

Fig. 10. Systematics of level spacings in the ground band (1) for odd-A rhodiums 107-113.

Fig. 11. Theoretical and experimental excitation energies of ^{111}Rh. The parameters used are $E(2^+) = 0.31MeV, \beta = 0.28$ and $\gamma = 28^\circ$ for ^{111}Rh.

Fig. 12. Theoretical and experimental excitation energies of ^{113}Rh. The parameters used are $E(2^+) = 0.3MeV, \beta = 0.27$ and $\gamma = 28^\circ$ for ^{113}Rh.

Fig. 13. Signature-splitting function S(I) of ^{111}Rh; dashed line-experiment, continuous line-theory.

Fig. 14. Signature-splitting function S(I) of ^{113}Rh; dashed line-experiment, continuous line-theory.

Fig. 15. Signature-splitting function S(I) of ^{110,112}Rh; solid and dashed lines are for the different isotopes, no theoretical calculation available for 2-quasiparticle systems.

TABLE I: Fission-gamma transitions in ^{111}Rh

E_γ	Rel. Int.	E_γ [9]	E_γ [8]	E_γ[7]	E_γ [3]	Band
78.57	3.2				78.7	8
91.41	1.3				91.3	5-8
107.42						1-6
136.75	2.9				136.9	5-8
161.24	1.5	161.4				1
161.79	12.3	161.8	161	162		7-6
172.45	2.9		173		172.6	5
185.54	0.5				185.5	5-8
189.0					188.8	
189.22					189.1	3-8
211.70	100	211.7	211	211	211.4	1
223.04	0.7				222.9	5
223.73		223.9	224			1
224.39		224.4	224	224		1
224.83	23.2	224.8	224	225		1
240.14	2.1		240		240.0	3
242.65	9.9	242.7	242	242		7
251.58	1.9	251.5	251			1
268.42	0.9				268.1	
279.67	31.2	279.7	279	280		1
295.44	5.1	295.4	295	295		7
303.69	23.8				303.6	8
313.58	4.3	313.6	313	313		7
316.02		316.0				1
354.38	3.9	354.4	354	354		6
355.43	0.9		355			5
355.66					355.7	5-1
361.03		361	361	361		7

TABLE I (cont.)

E_γ	Rel. Int.	E_γ [9]	E_γ [8]	E_γ[7]	E_γ [3]	Band
377.82	3.2	377.8	378			1
381.79	0.5					5
382.21	7.2				382.0	8
395.1	0.3				395.0	5
397.15	23.3	397.1	397	397		6-1
402.04	4.1	402.0	402.0	402		6
409.54		409.4				1
410.76	16.9	410.8	411	411		6
417.22						7
435.63	1.3		436			3
442.86	12.8	442.9	442	443		1
491.36	14.8	491.4	491	491		1
504.49	22.8	504.5	504	504		1
522.53	0.7		522			5
529.31	4.7	529.3	529	529		6
538.14	1.3			538		7
539.22		539.2				1
549.53	3.5	549.4	550	549		1
567.65					567.5	5
576.32	1.2	576.4				1
576.94	6.5	576.9	577	577		6
589.56	0.9		591			3
608.76	1.5					6
609.06	1.2			608		7
629.34	1.8	629.3				1
653.29	2.0	653.3				6
657.66	2.3	657.8	658	658		6-1
661.01	0.6	660.9				1

TABLE I (cont.)

E_γ	Rel. Int.	E_γ [9]	E_γ [8]	E_γ[7]	E_γ [3]	Band
667.32	9.1	667.3	667	667		1
667.68	6.6	667.7	667.0	668		1
668.33	0.6		668			5
674.66	0.8			675		7
725.35	1.1	725.4				1
729.32	1.3	729.2				7-1
737.79	6.6	737.8	738			1
765.36	5.5	765.2	765	765		6
773.26	7.4	773.3	774			1
773.84	1.7	773.8	774	773		1
778.0						7
791.34	0.4					5
791.94	3.7	791.8	792	792		6-1
800.4	0.6	800.3				1
807.72	0.4					6-1
882.81	1.2			883		6-1

TABLE II: Fission-gamma transitions in ^{113}Rh

E_γ	Rel. Int.	E_γ [9]	E_γ [8]	E_γ[4]	Band
88.17	5.4			88.1	8
185.82	4.5			185.8	5
206.10	0.6			206.2	3-8
211.70	100	212	212	211.7	1
227.68	0.7			227.6	8
232.28	20.7	232	232	232.3	1
233.69	2.2			233.9	5
236.0					1
240.65	15.8	241	240		1
244.0					1
244.48	7.3	245	245		1
252.95	1.1	253			1
262.55	2.2	262			1
263.17	20.3			263.2	8
313.35	2.7	313			2
315.73					8
330.45	0.9				2
332.97	0.3				5
337.58	5.1			337.6	5-8
347.84	2.6	348	348		6
351.44	6.9			351.2	8
351.65	1.3				6
356.1					2
357.67	5.1	358			2-1
359.26	6.2	359	358		6-1
365.33	5.2	366	365		6
367.25	0.2			367.1	8-1

TABLE II (cont.)

E_γ	Rel. Int.	E_γ [9]	E_γ [8]	E_γ[4]	Band
367.67	1.0	368			1
373.09	0.5				6
389.36	1.7	389			6
391.18	8.4	391	391		1
424.26	1.2				5
432.26	1.9	433			1
433.82					3-8
435.24					1
443.95	18.9	444	444	443.9	1
455.34	6.6	455	454		1
472.93	19.3	473	472		1
483.04	0.6			482.0	5-8
560.54					8
571.0	0.9				6
571.07	1.8			571.1	5-8
599.45	1.2	600			6-1
600.7	0.7			600.5	5
611.45	0.5	612			1
620.35	0.4	621			1
631.65	5.2	632	631		1
635.55	14.4	636	636		1
643.66	0.5				2
671.27	0.3				1
679.33	0.3				1
685.32	1.6	686			1
686.57	0.3	687			2
694.87	1.4	695			1
699.76	2.5	700	699		1

TABLE II (cont.)

E_γ	Rel. Int.	E_γ [9]	E_γ [8]	E_γ[4]	Band
713.40	0.6	714			6
717.66	5.0	717	718		1
724.60	2.2	725			6-1
724.95	0.3				6
737.34	1.1	737	476		6
740.95	0.3				6
785				785.0	3
840.3					6-1
949.61	0.9				6-1

TABLE III: Fission-gamma transitions in ^{110}Rh

E_γ	Rel. Int.	E_γ [7]02	E_γ [7]03	Band
58.88	$>$ 180			1
65.82	$>$ 130			1
159.26	100		159.1	1
186.80	53.1	187	186.6	1
258.02	13.1	258	257.8	1
299.88	23.9	300	299.5	1
346.14	1.3			1
362.34	7.9	362	362.2	1
375.34	2.8	375	374.8	1
486.65	5.6	486	486.0	1
557.85	5.9	558	557.5	1
620.33	10.9	620	620.1	1
737.54	1.4	737	737.3	1

TABLE IV: Fission-gamma transitions in ^{112}Rh

E_γ	Rel. Int.	E_γ [9]	E_γ [7]02	E_γ [7]03	Band
60.58	> 200				1
159.16	100	159		158.9	1
183.03	55.9	183	183	182.8	1
241.98	8.4	242	242	241.7	1
268.55	29.5	269	268	268.3	1
327.96	6.9	328	328	327.8	1
335.4					1
342.42	3.7				1
343.68	2.0	343			1
362.43	3.1	363	362	362.1	1
399.66	3.1	400			2-1
427.52	1.5	427			2
451.46	5.1		451	451.2	1
486.47	1.6	487			1
510.7		511	510.0	510.2	1
569.86	10.3	570	570	569.7	1
690.56	5.1	691	690	690.2	1
706.08	4.4	706			1
821.77		822			1
830.10		830			1

TABLE V: Gamma Ray Energy Difference Tests in ^{111}Rh

Gamma 1	Gamma 2	Diff.	Ref.	Comments
382.0	170.6	211.4	Lherssoneau98	
567.5	355.7	211.8	Lherssoneau98	
632.4	420.9	211.5	Lherssoneau98	
1038.9	827.4	211.5	Lherssoneau98	
1898.1	1686.3	211.8	Lherssoneau98	weak
2034.1	1822.3	211.8	Lherssoneau98	
490.7	279.2	211.5	Venkova02	
491.36	279.67	211.69	Present work	
608.76	397.15	211.61	Present work	weak
567.65	355.66	211.99	Present work	weak

TABLE VI: Gamma-ray intensity ratios; spins without index refer to yrast states

Ratio	^{111}Rh		^{113}Rh	
	theory	exp.	theory	exp.
$I(11/2 \rightarrow 9/2)/I(11/2 \rightarrow 7/2)$	1.33	2.1	1.3	1.1
$I(13/2 \rightarrow 11/2/I(13/2 \rightarrow 9/2)$	0.45	1	0.80	0.84
$I(15/2 \rightarrow 13/2)I(15/2 \rightarrow 11/2)$	0.82	1.9	0.66	1.61
$I(11/2_2 \rightarrow 9/2)/I(11/2_2 \rightarrow 7/2)$	10.0	15.5	6	6.9

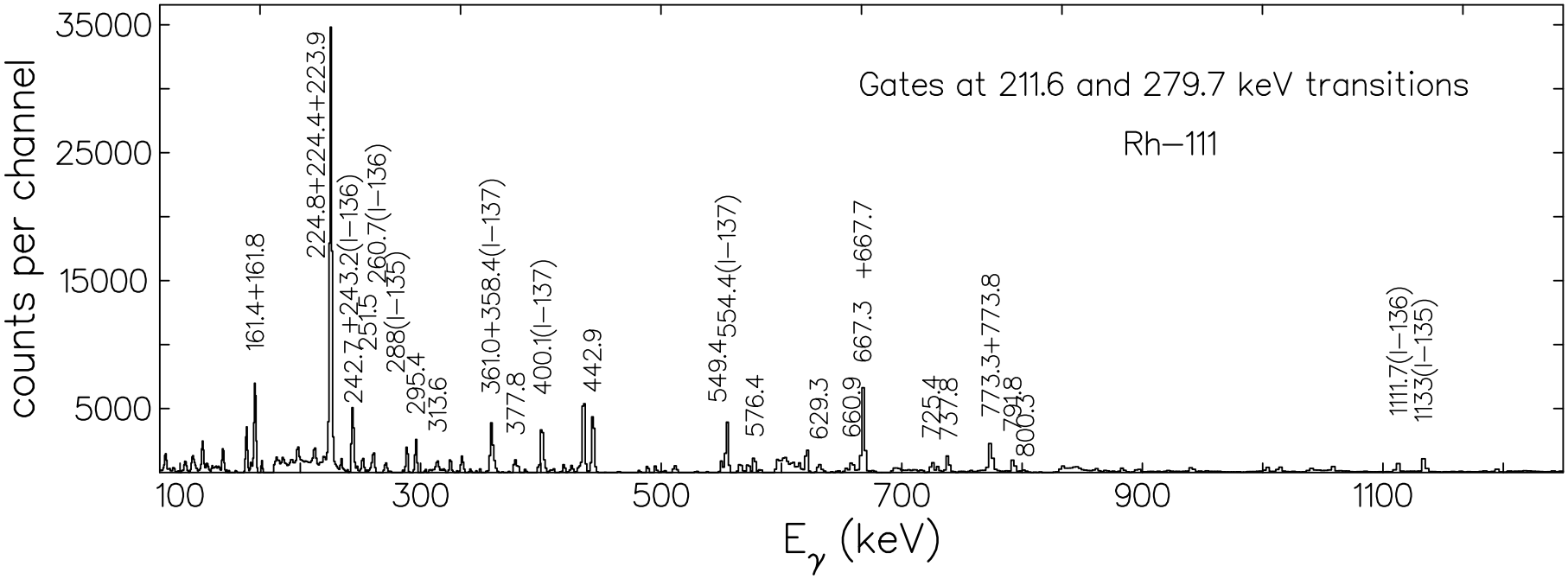
Gates at 211.6 and 279.7 keV transitions
Rh–111
counts per channel
E$_\gamma$ (keV)
35000
25000
15000
5000
100
300
500
700
900
1100
161.4+161.8
224.8+224.4+223.9
242.7+243.2(I–136)
251.5
260.7(I–136)
288(I–135)
295.4
313.6
361.0+358.4(I–137)
377.8
400.1(I–137)
442.9
549.4
554.4(I–137)
576.4
629.3
660.9
667.3
+667.7
725.4
737.8
773.3+773.8
791.8
806.3
1111.7(I–136)
1133(I–135)

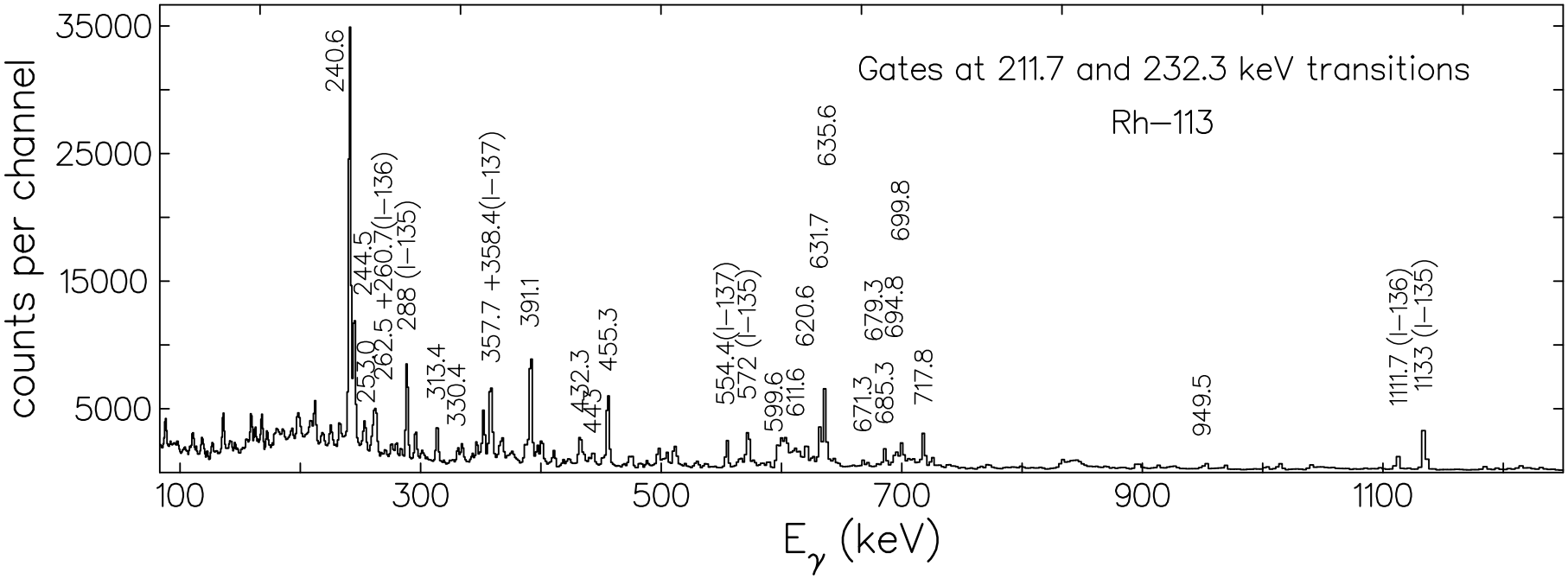
Gates at 211.7 and 232.3 keV transitions
Rh–113
counts per channel
E_γ (keV)
35000
25000
15000
5000
100
300
500
700
900
1100
240.6
253.0
244.5
262.5 +260.7(I–136)
288 (I–135)
313.4
330.4
357.7 +358.4(I–137)
391.1
432.3
443
455.3
554.4(I–137)
572 (I–135)
599.6
611.6
620.6
631.7
635.6
671.3
685.3
679.3
694.8
699.8
717.8
949.5
1111.7 (I–136)
1133 (I–135)

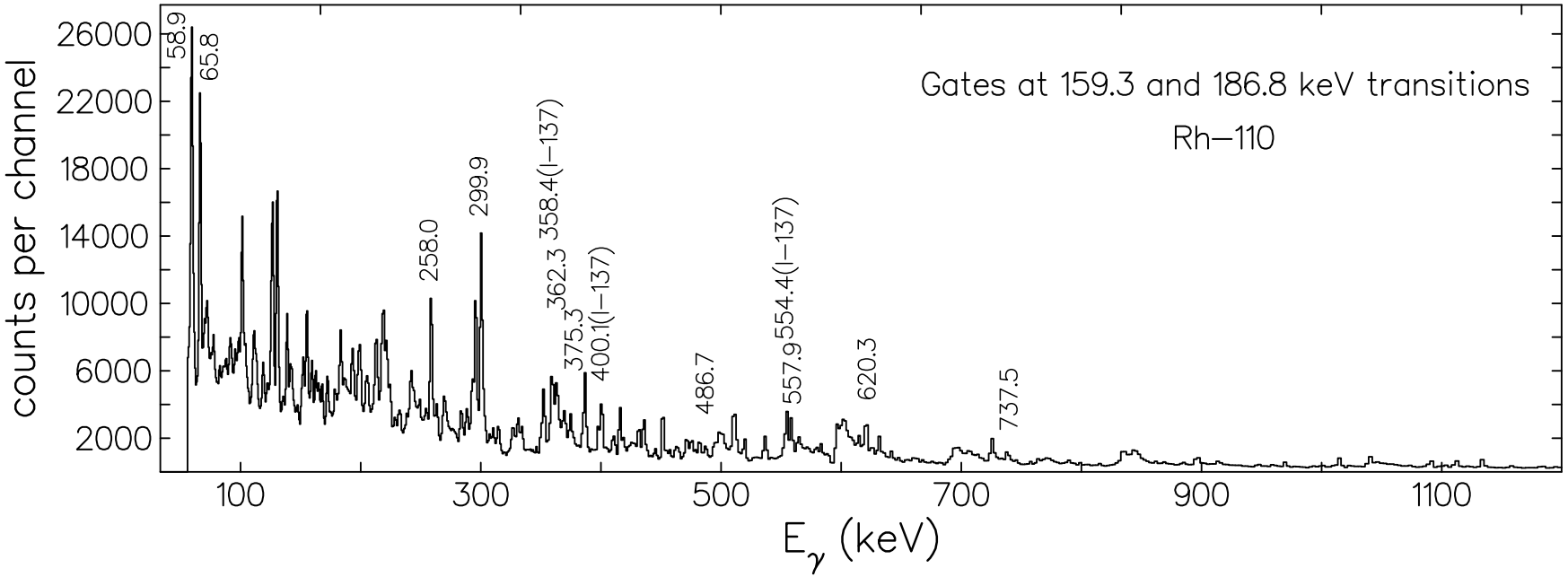
Gates at 159.3 and 186.8 keV transitions
Rh–110
counts per channel
26000
22000
18000
14000
10000
6000
2000
100
300
500
700
900
1100
E_γ (keV)
58.9
65.8
258.0
299.9
358.4(I–137)
362.3
375.3
400.1(I–137)
486.7
554.4(I–137)
557.9
620.3
737.5

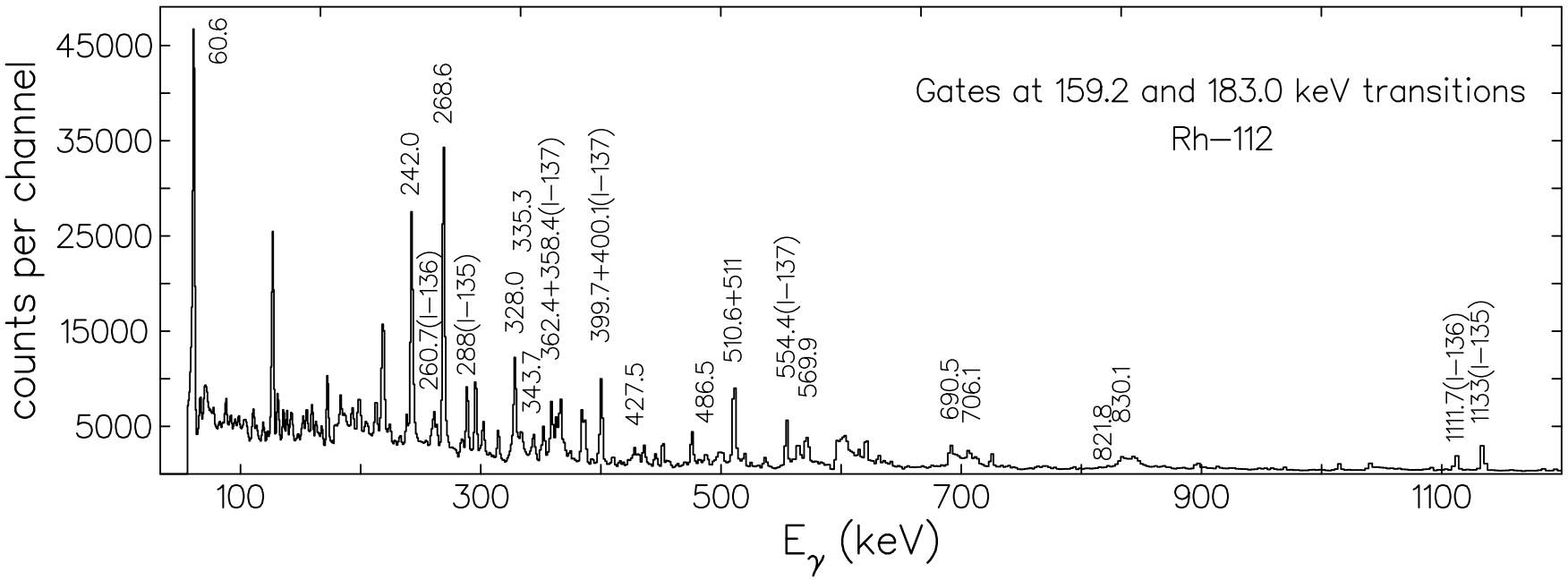
Gates at 159.2 and 183.0 keV transitions
Rh–112
counts per channel
45000
35000
25000
15000
5000
100
300
500
700
900
1100
E_γ (keV)
60.6
242.0
260.7(I–136)
268.6
288(I–135)
328.0
335.3
343.7
362.4+358.4(I–137)
399.7+400.1(I–137)
427.5
486.5
510.6+511
554.4(I–137)
569.9
690.5
706.1
821.8
830.1
1111.7(I–136)
1133(I–135)

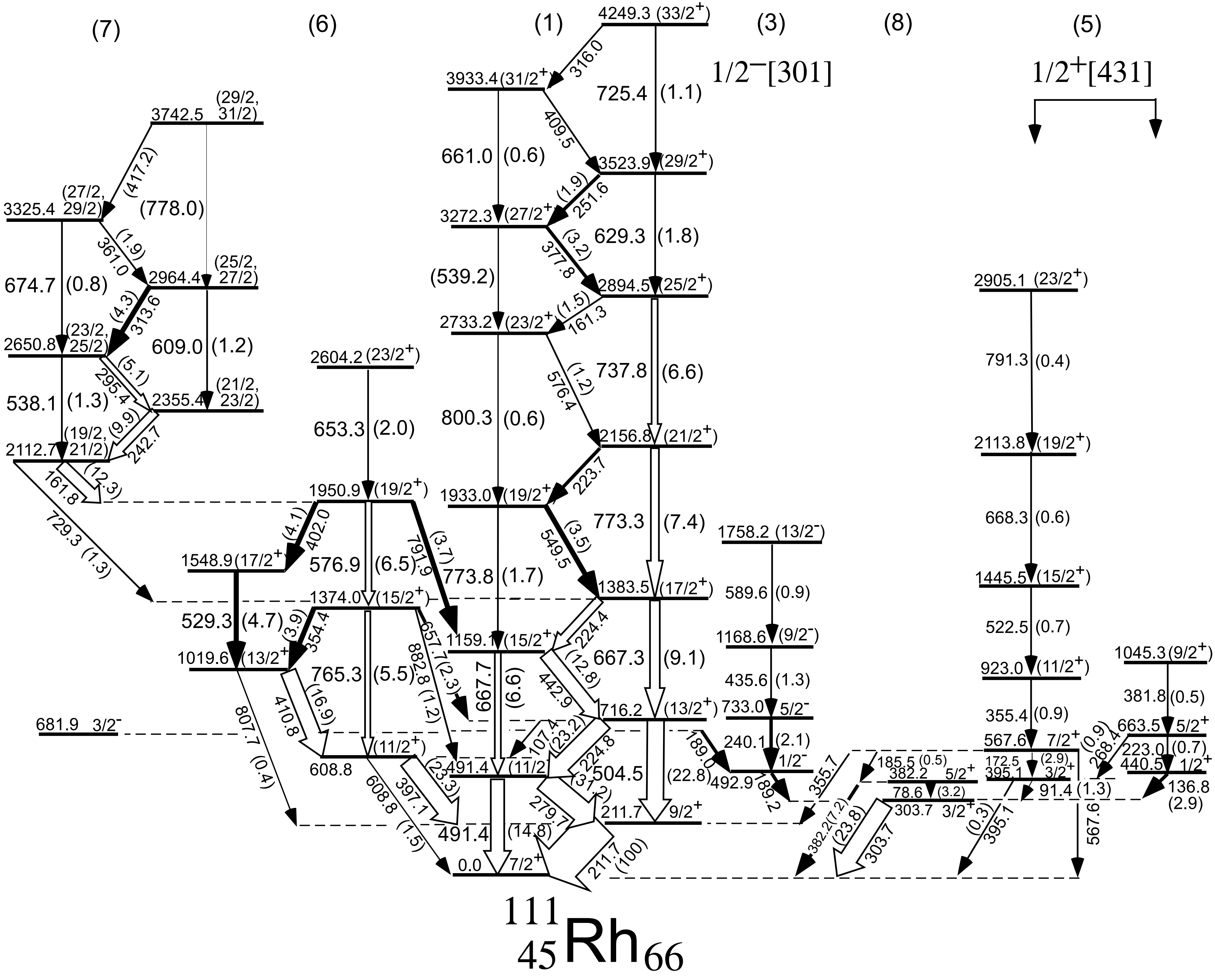
(7)
(6)
(1)
(3)
(8)
(5)
1/2⁻[301]
1/2⁺[431]
4249.3 (33/2⁺)
3933.4 (31/2⁺)
3523.9 (29/2⁺)
3272.3 (27/2⁺)
2894.5 (25/2⁺)
2733.2 (23/2⁺)
2156.8 (21/2⁺)
1933.0 (19/2⁺)
1383.5 (17/2⁺)
1159.1 (15/2⁺)
716.2 (13/2⁺)
491.4 (11/2⁺)
211.7 9/2⁺
0.0 7/2⁺
3742.5 (29/2, 31/2)
3325.4 (27/2, 29/2)
2964.4 (25/2, 27/2)
2650.8 (23/2, 25/2)
2355.4 (21/2, 23/2)
2112.7 (19/2, 21/2)
2604.2 (23/2⁺)
1950.9 (19/2⁺)
1548.9 (17/2⁺)
1374.0 (15/2⁺)
1019.6 (13/2⁺)
608.8 (11/2⁺)
681.9 3/2⁻
1758.2 (13/2⁻)
1168.6 (9/2⁻)
733.0 5/2⁻
492.9 1/2⁻
382.2 5/2⁺
303.7 3/2⁺
2905.1 (23/2⁺)
2113.8 (19/2⁺)
1445.5 (15/2⁺)
923.0 (11/2⁺)
567.6 7/2⁺
395.1 3/2⁺
1045.3 (9/2⁺)
663.5 5/2⁺
440.5 1/2⁺
316.0
725.4 (1.1)
661.0 (0.6)
409.5
629.3 (1.8)
(1.9) 251.6
(3.2) 377.8
(539.2)
(1.5) 161.3
737.8 (6.6)
(1.2) 576.4
800.3 (0.6)
223.7
773.3 (7.4)
(3.5) 549.5
773.8 (1.7)
224.4
667.3 (9.1)
(12.8) 442.9
667.7 (6.9)
107.4 (23.2)
224.8 (31.2)
504.5
(22.8)
279.7 (14.8)
491.4
211.7 (100)
189.0
(417.2)
(778.0)
(1.9) 361.0
674.7 (0.8)
(4.3) 313.6
609.0 (1.2)
(5.1) 295.4
538.1 (1.3)
(9.9) 242.7
161.8 (12.3)
729.3 (1.3)
653.3 (2.0)
(4.1) 402.0
576.9 (6.5)
(3.7) 791.9
529.3 (4.7)
(3.9) 354.4
765.3 (5.5)
657.7 (2.3)
882.8 (1.2)
410.8 (16.9)
807.7 (0.4)
608.8 (1.5)
397.1 (23.3)
589.6 (0.9)
435.6 (1.3)
240.1 (2.1)
189.2
355.7
185.5 (0.5)
78.6 (3.2)
382.2 (7.2)
(23.8) 303.7
791.3 (0.4)
668.3 (0.6)
522.5 (0.7)
355.4 (0.9)
172.5 (2.9)
91.4 (1.3)
(0.3) 395.1
567.6
381.8 (0.5)
(0.9) 268.4
223.0 (0.7)
136.8 (2.9)
111 45 Rh 66

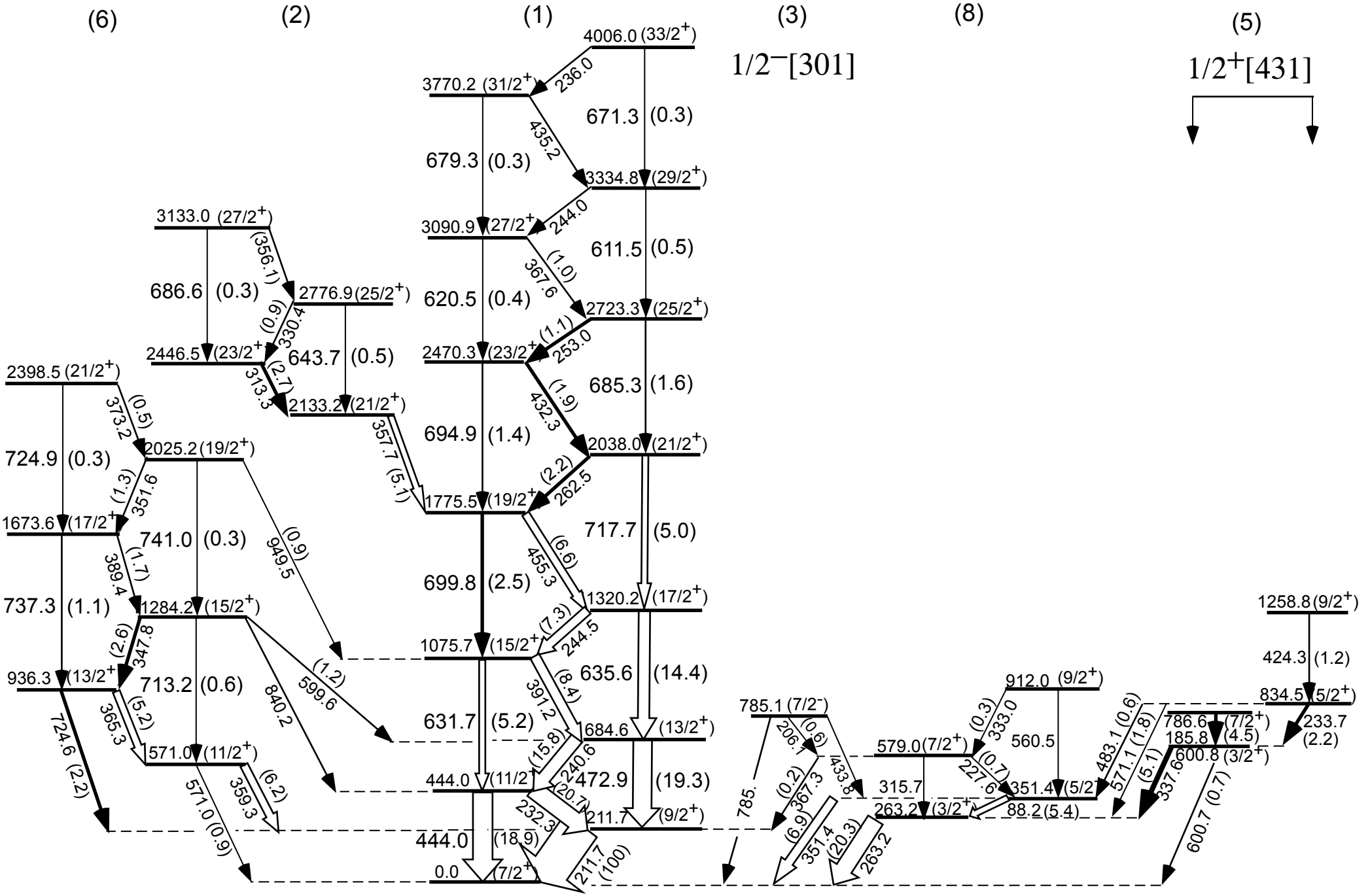
(6)
(2)
(1)
(3)
(8)
(5)
1/2−[301]
1/2+[431]
4006.0 (33/2+)
3770.2 (31/2+)
3334.8 (29/2+)
3133.0 (27/2+)
3090.9 (27/2+)
2776.9 (25/2+)
2723.3 (25/2+)
2446.5 (23/2+)
2470.3 (23/2+)
2398.5 (21/2+)
2133.2 (21/2+)
2038.0 (21/2+)
2025.2 (19/2+)
1775.5 (19/2+)
1673.6 (17/2+)
1320.2 (17/2+)
1284.2 (15/2+)
1075.7 (15/2+)
936.3 (13/2+)
684.6 (13/2+)
571.0 (11/2+)
444.0 (11/2−)
444.0 (18.9)
0.0 (7/2+)
211.7 (9/2+)
785.1 (7/2−)
912.0 (9/2+)
579.0 (7/2+)
315.7
263.2 (3/2+)
351.4 (5/2+)
88.2 (5.4)
1258.8 (9/2+)
834.5 (5/2+)
786.6 (7/2+)
600.8 (3/2+)
185.8 (4.5)
233.7 (2.2)
424.3 (1.2)
236.0
671.3 (0.3)
435.2
679.3 (0.3)
244.0
611.5 (0.5)
367.6 (1.0)
620.5 (0.4)
253.0 (1.1)
685.3 (1.6)
432.3 (1.9)
694.9 (1.4)
262.5 (2.2)
717.7 (5.0)
455.3 (6.6)
699.8 (2.5)
244.5 (7.3)
635.6 (14.4)
391.2 (8.4)
631.7 (5.2)
240.6 (15.8)
472.9 (19.3)
232.3 (20.7)
211.7 (100)
686.6 (0.3)
356.1 (6.0)
330.4 (2.7)
643.7 (0.5)
313.3
357.7 (5.1)
373.2 (0.5)
724.9 (0.3)
351.6 (1.3)
741.0 (0.3)
389.4 (1.7)
949.5 (0.9)
737.3 (1.1)
347.8 (2.6)
599.6 (1.2)
713.2 (0.6)
365.3 (5.2)
840.2
724.6 (2.2)
359.3 (6.2)
571.0 (0.9)
785.
206.1 (0.6)
433.8
(0.2)
367.3 (6.9)
351.4 (20.3)
263.2
333.0 (0.3)
560.5
227.6 (0.7)
88.2 (5.4)
483.1 (0.6)
571.1 (1.8)
337.6 (5.1)
600.7 (0.7)

$^{113}_{45}Rh_{68}$

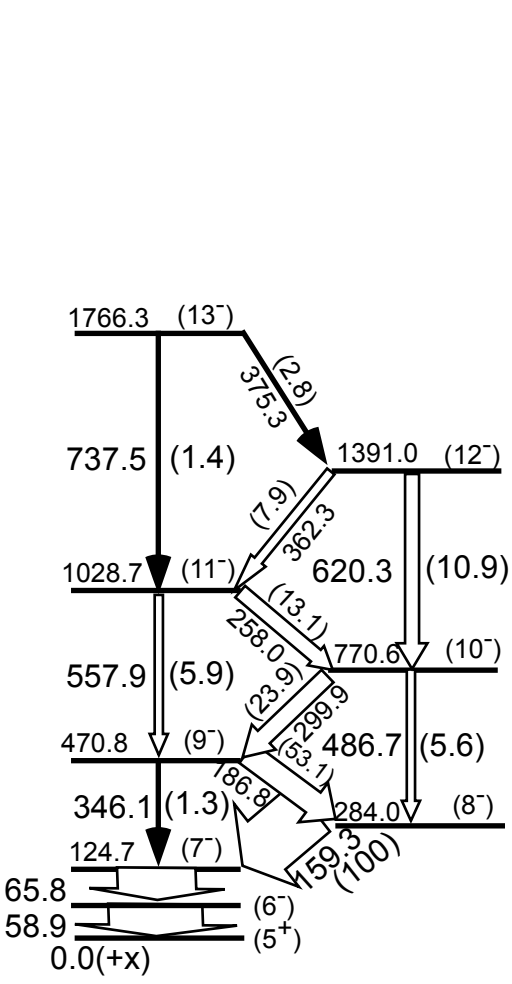

$^{110}_{45}Rh_{65}$

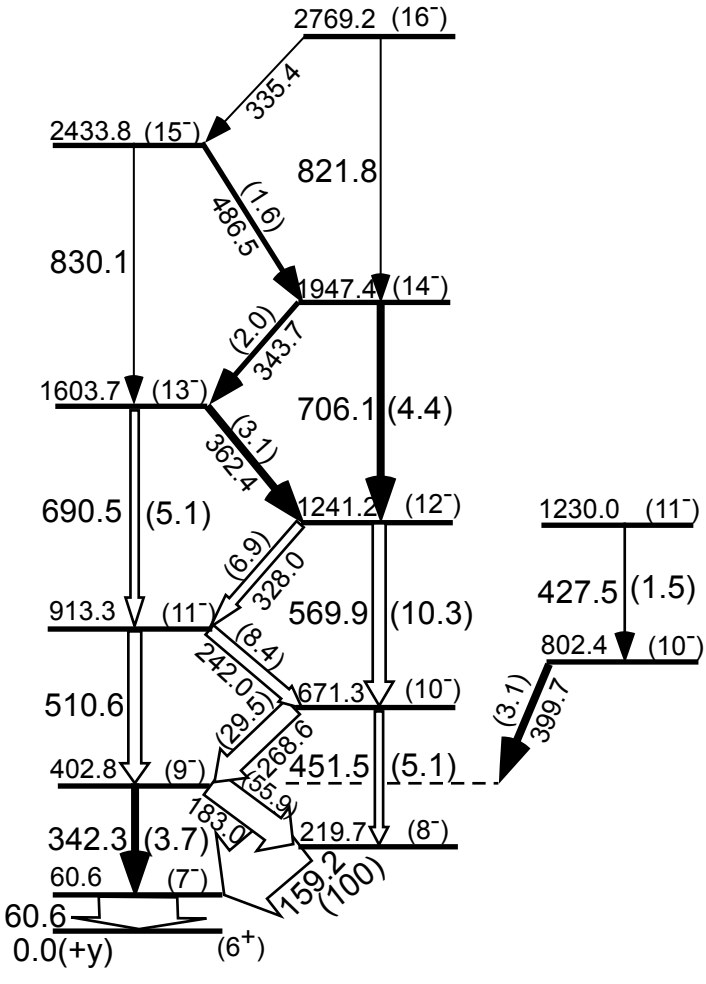

$^{112}_{45}Rh_{67}$

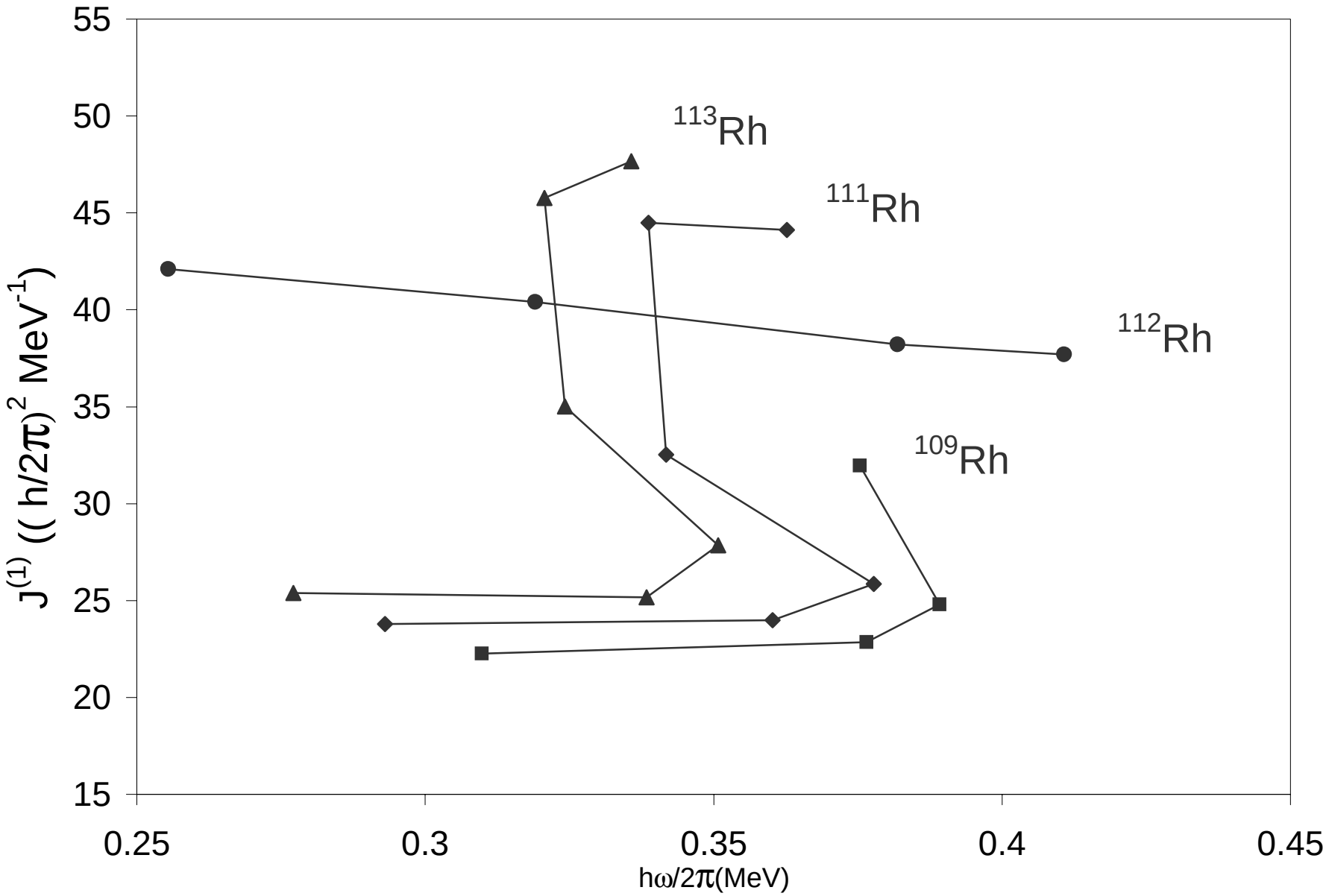
55
50
45
40
35
30
25
20
15
0.25
0.3
0.35
0.4
0.45
$J^{(1)}$ ((h/2π)^2 MeV^{-1})
hω/2π(MeV)
^{113}Rh
^{111}Rh
^{112}Rh
^{109}Rh

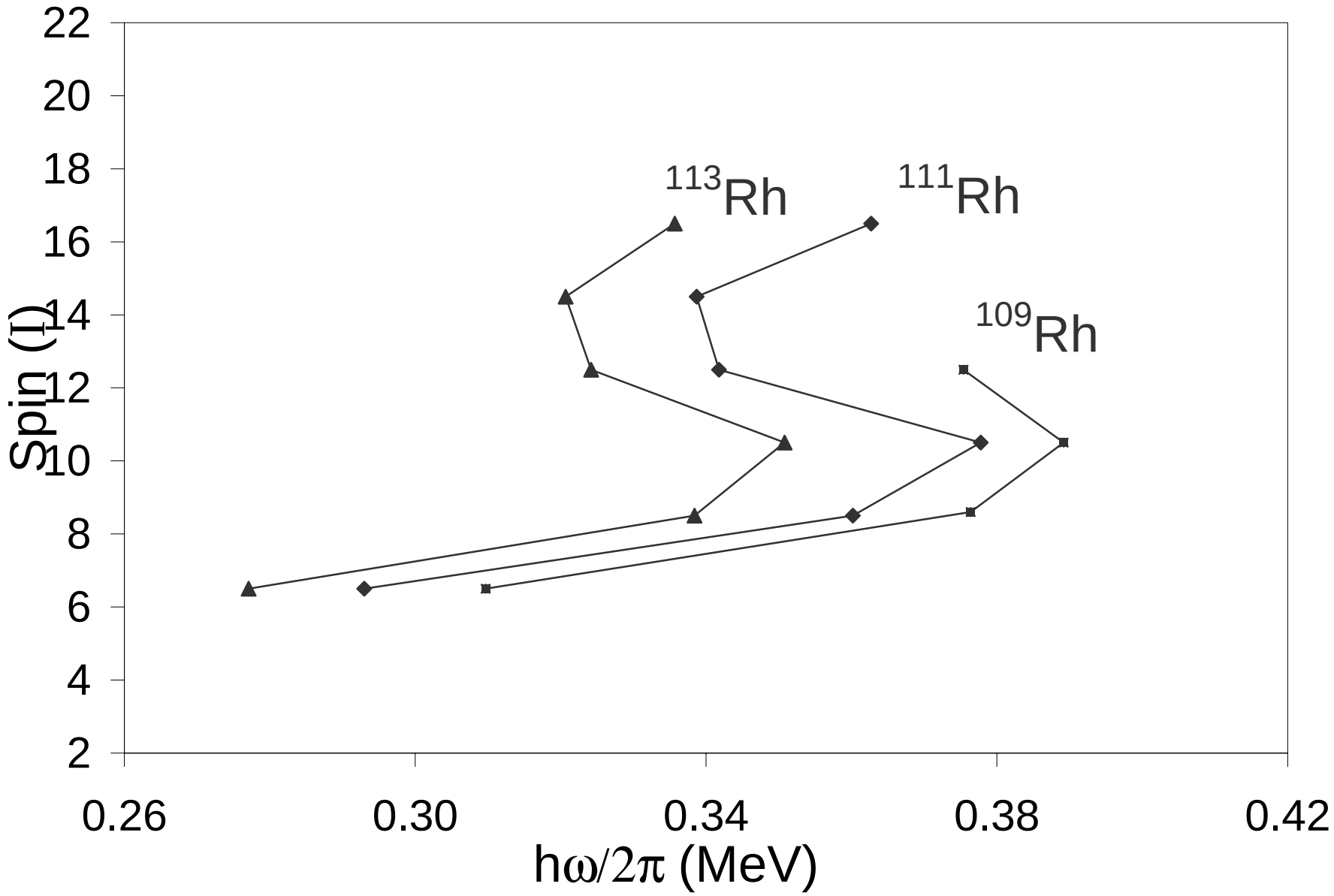
22
20
18
16
14
12
10
8
6
4
2
Spin (I)
^{113}Rh
^{111}Rh
^{109}Rh
0.26
0.30
0.34
0.38
0.42
hω/2π (MeV)

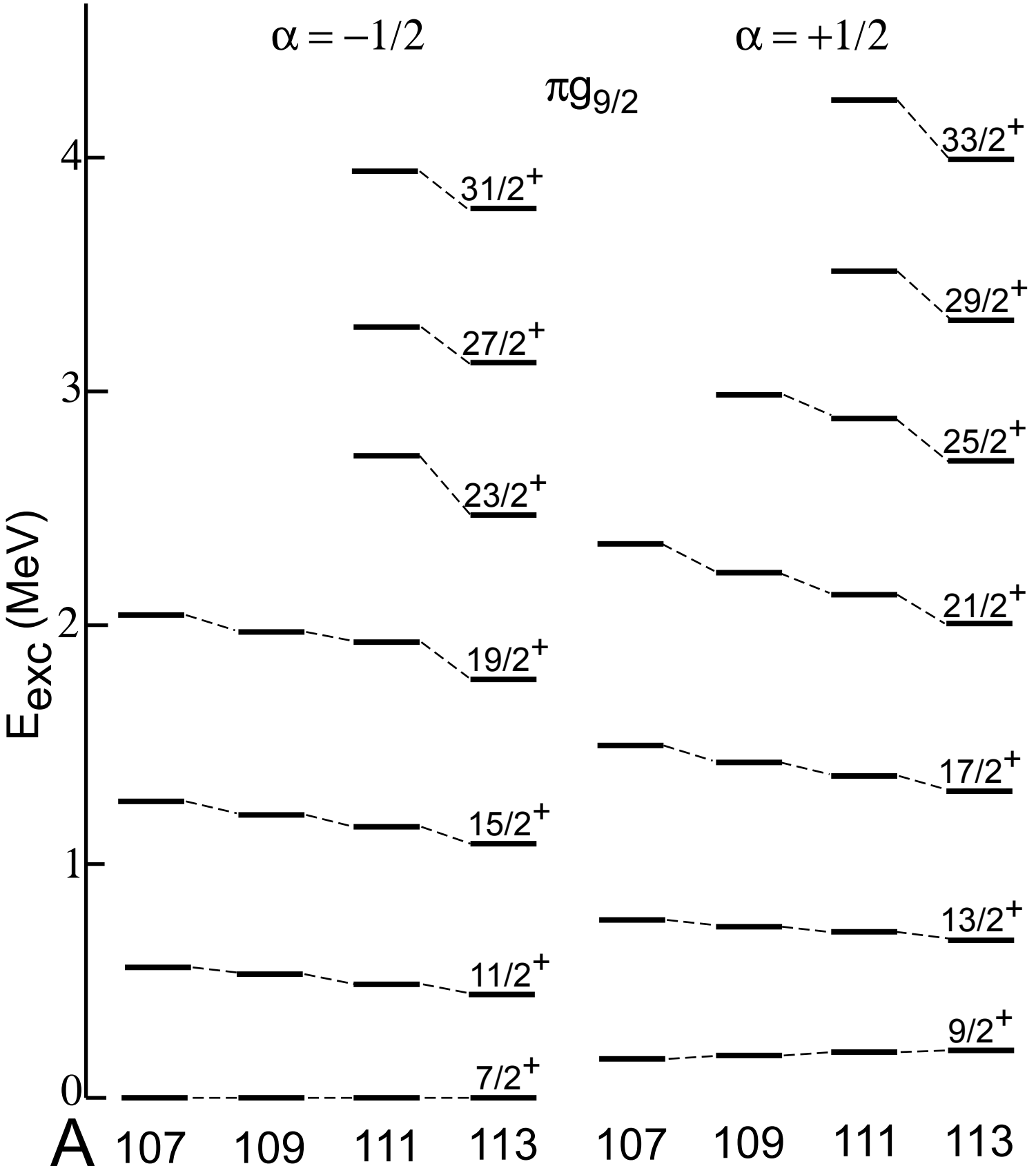
α = −1/2
α = +1/2
πg9/2
33/2+
31/2+
29/2+
27/2+
25/2+
23/2+
21/2+
19/2+
17/2+
15/2+
13/2+
11/2+
9/2+
7/2+
Eexc (MeV)
0
1
2
3
4
A
107
109
111
113
107
109
111
113

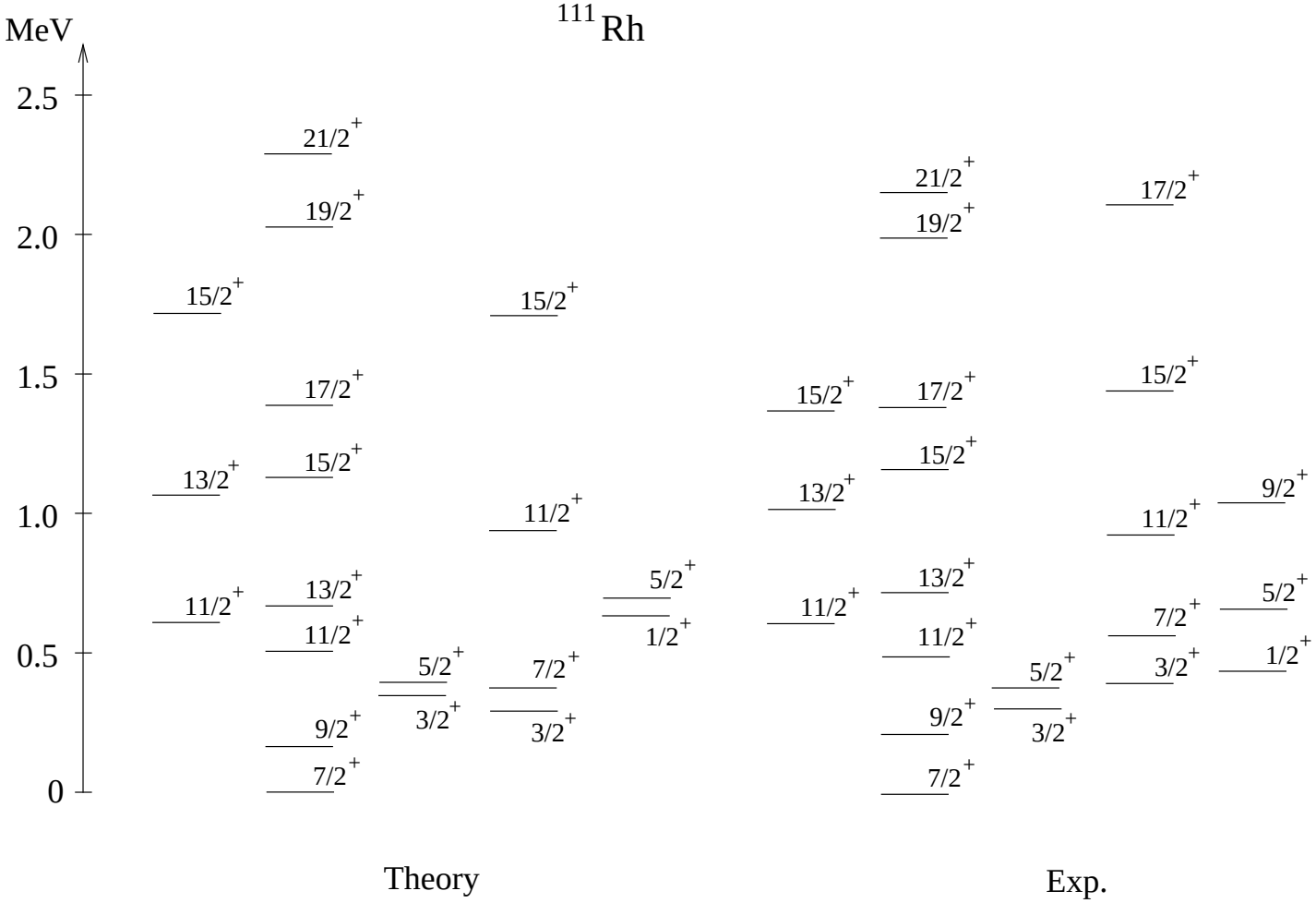
^{111}Rh
MeV
2.5
2.0
1.5
1.0
0.5
0
21/2+
19/2+
15/2+
17/2+
15/2+
13/2+
11/2+
13/2+
11/2+
9/2+
7/2+
5/2+
3/2+
15/2+
11/2+
7/2+
3/2+
5/2+
1/2+
Theory
21/2+
19/2+
15/2+
17/2+
15/2+
13/2+
11/2+
13/2+
11/2+
9/2+
7/2+
5/2+
3/2+
17/2+
15/2+
11/2+
9/2+
7/2+
3/2+
5/2+
1/2+
Exp.

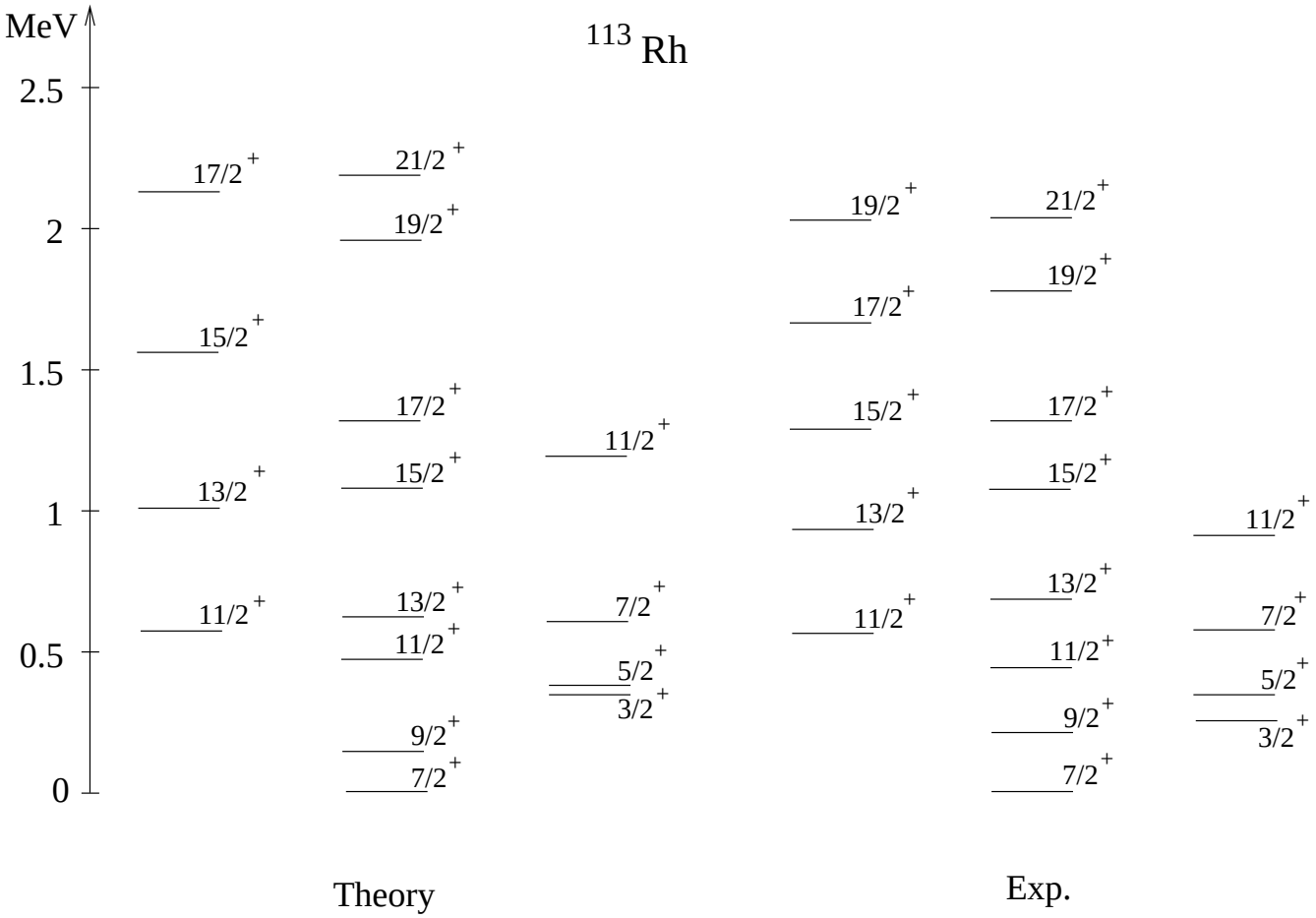
MeV
^{113}Rh
2.5
2
1.5
1
0.5
0
17/2+
15/2+
13/2+
11/2+
21/2+
19/2+
17/2+
15/2+
13/2+
11/2+
9/2+
7/2+
11/2+
7/2+
5/2+
3/2+
19/2+
17/2+
15/2+
13/2+
11/2+
21/2+
19/2+
17/2+
15/2+
13/2+
11/2+
9/2+
7/2+
11/2+
7/2+
5/2+
3/2+
Theory
Exp.

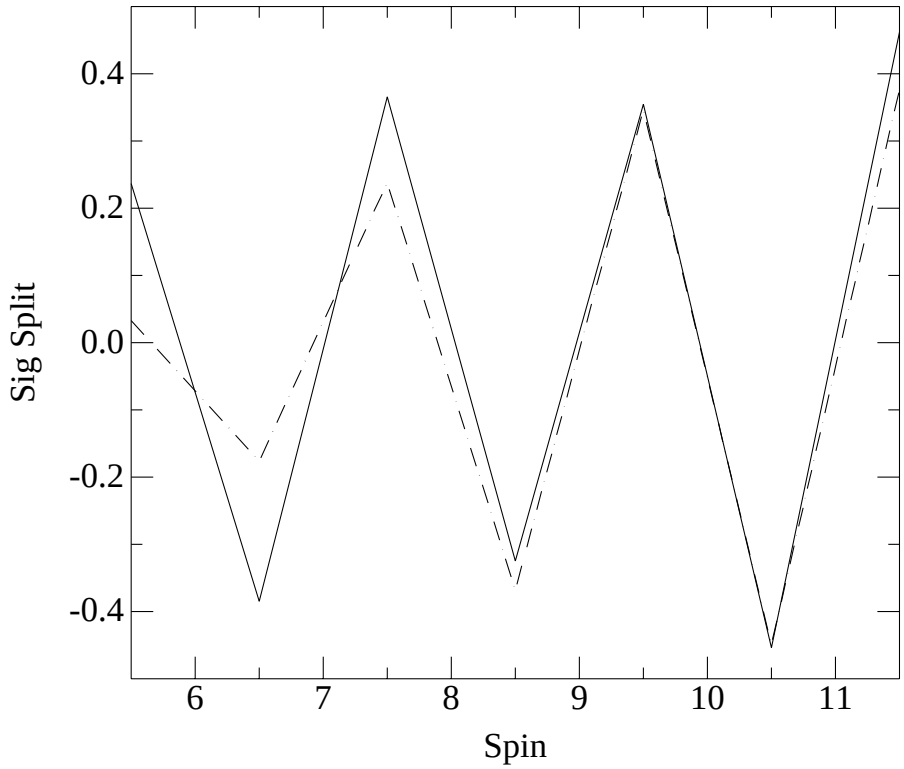
0.4
0.2
0.0
-0.2
-0.4
Sig Split
6
7
8
9
10
11
Spin

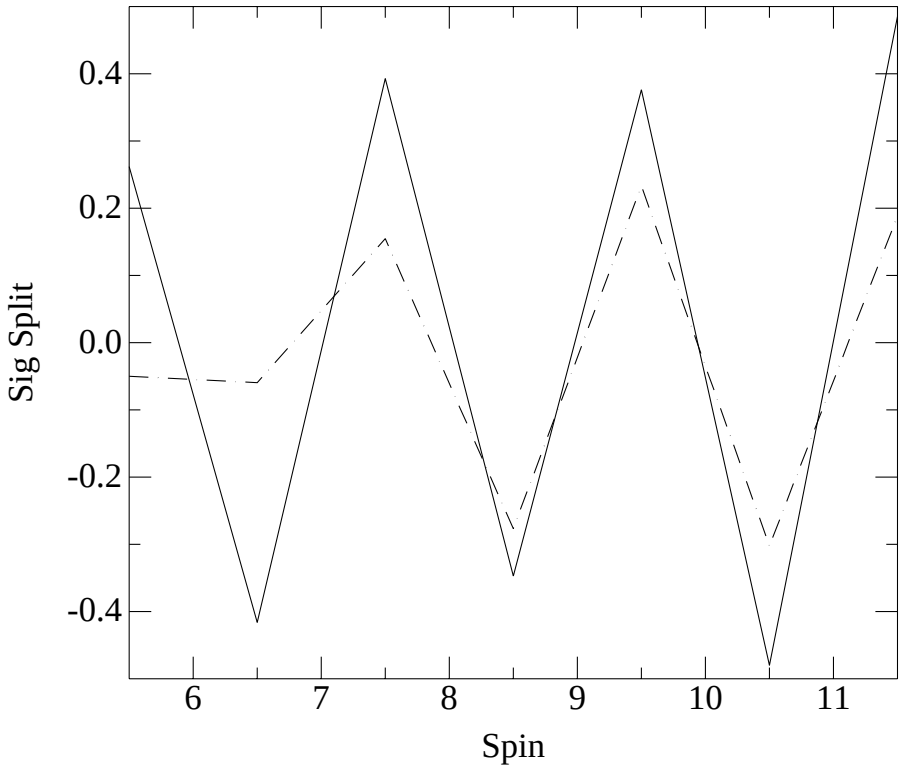
0.4
0.2
0.0
-0.2
-0.4
Sig Split
6
7
8
9
10
11
Spin

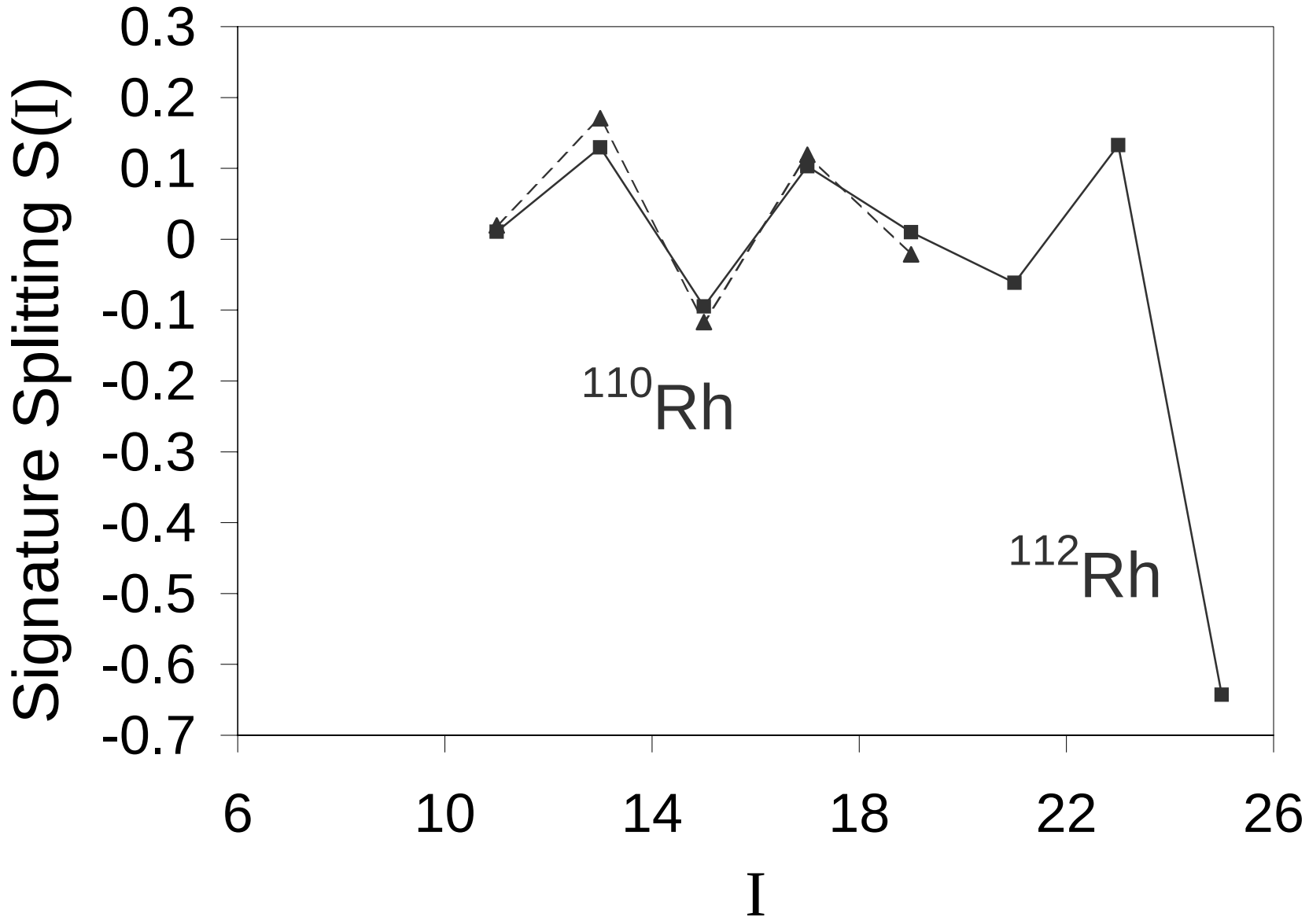
Signature Splitting S(I)
0.3
0.2
0.1
0
-0.1
-0.2
-0.3
-0.4
-0.5
-0.6
-0.7
6
10
14
18
22
26
I
110Rh
112Rh